

Some analytical approaches for large-scale structures

Patrick Valageas

Institut de Physique Théorique, CEA Saclay

Outline

- Perturbative methods
- Eulerian / Lagrangian frameworks
- Exact results for toy models: adhesion model
- Combined models
- Spherical collapse
- Halo mass function
- Probability distribution of the density contrast
- Modified gravity

Perturbative methods

$$x > 10h^{-1}\text{Mpc}$$

Scales of interest:

$$k < 0.4h\text{Mpc}^{-1}$$

Linear to weakly nonlinear regime

Future observations require a percent-level accuracy
for theoretical predictions

F. Bernardeau & P.V., 2008 - P.V., 2004; 2007a,b; 2008; 2010a - P.V. & T. Nishimichi, 2011 - Ph. Brax & P.V. 2012

F. Bernardeau, M. Crocce, E. Sefusatti; 2010 - M. Crocce & R. Scoccimarro, 2006a,b; 2008 - S. Matarrese & M. Pietroni, 2007 - M. Pietroni, 2008 - A. Taruya & T. Hiramatsu, 2008

A- Standard perturbation theory

I) Hydrodynamical approximation (single-stream approximation)

(C)DM+baryons: (pressure-less)
& irrotational perfect fluid

$$\frac{\partial \delta}{\partial \tau} + \nabla \cdot [(1 + \delta) \mathbf{v}] = 0$$

density contrast:

$$\frac{\partial \mathbf{v}}{\partial \tau} + \mathcal{H} \mathbf{v} + (\mathbf{v} \cdot \nabla) \mathbf{v} = -\nabla \Phi - c_s^2 \frac{\nabla \rho}{\bar{\rho}}$$

$$\delta(\mathbf{x}, t) = \frac{\rho(\mathbf{x}, t) - \bar{\rho}}{\bar{\rho}}$$

$$\Delta \phi = \frac{3}{2} \Omega_m \mathcal{H}^2 \delta$$

2) Solution as a perturbative expansion over powers of the linear mode

$$\tilde{\delta}(\mathbf{k}, \tau) = \sum_{n=1}^{\infty} \tilde{\delta}^{(n)}(\mathbf{k}, \tau) \quad \text{with} \quad \tilde{\delta}^{(n)} \propto (\tilde{\delta}_L)^n$$

3) Gaussian average for statistical quantities

$$C_2 = \langle \delta \delta \rangle = \langle \delta^{(1)} \delta^{(1)} \rangle + \langle \delta^{(3)} \delta^{(1)} \rangle + \langle \delta^{(1)} \delta^{(3)} \rangle + \langle \delta^{(2)} \delta^{(2)} \rangle + \dots$$

Using the Poisson equation, one obtains 2 equations for the density and velocity fields, which are quadratic.

Introduce the velocity divergence: $\theta = \nabla \cdot \mathbf{v}$

a 2-component vector: $\psi = \begin{pmatrix} \delta \\ -\theta/\dot{a} \end{pmatrix}$

Quadratic equation of motion, with a linear operator that may depend on wavenumber (pressure-like term or modified gravity):

$$\mathcal{O} \cdot \tilde{\psi} = K_s \cdot \tilde{\psi} \tilde{\psi}$$

$$\mathcal{O} = \begin{pmatrix} \frac{\partial}{\partial \ln a} & -1 \\ -\frac{3\Omega_m}{2}[1 + \epsilon(k, a)] & \frac{\partial}{\partial \ln a} + \frac{1-3w\Omega_{de}}{2} \end{pmatrix}$$

WDM pressure-like term: $\epsilon(k, a) = -\frac{k^2}{k_{fs}(a)^2}$

Modified gravity: $\epsilon(k, a) = \frac{2\beta(a)^2 k^2}{k^2 + m(a)^2 a^2}$

$$\mathcal{O} \cdot \tilde{\psi} = K_s \cdot \tilde{\psi} \tilde{\psi}$$

Standard perturbative expansion: $\tilde{\psi}(x) = \sum_{n=1}^{\infty} \tilde{\psi}^{(n)}(x)$ with $\tilde{\psi}^{(n)} \propto (\tilde{\psi}_L)^n$

solved by recursion up to the required order n :

$$\mathcal{O} \cdot \tilde{\psi}^{(n)} = K_s(x; x_1, x_2) \sum_{\ell=1}^{n-1} \tilde{\psi}^{(\ell)}(x_1) \tilde{\psi}^{(n-\ell)}(x_2)$$

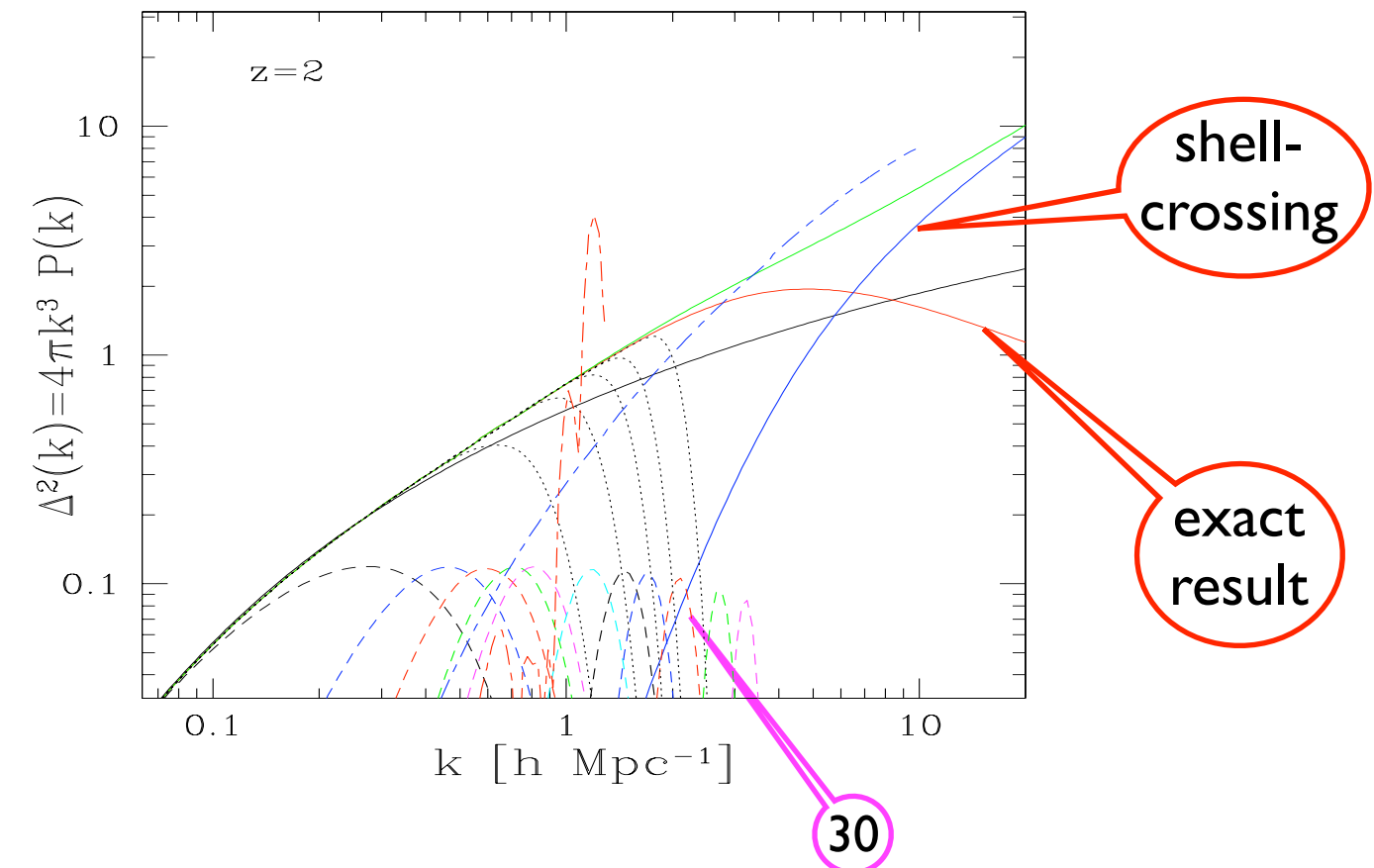
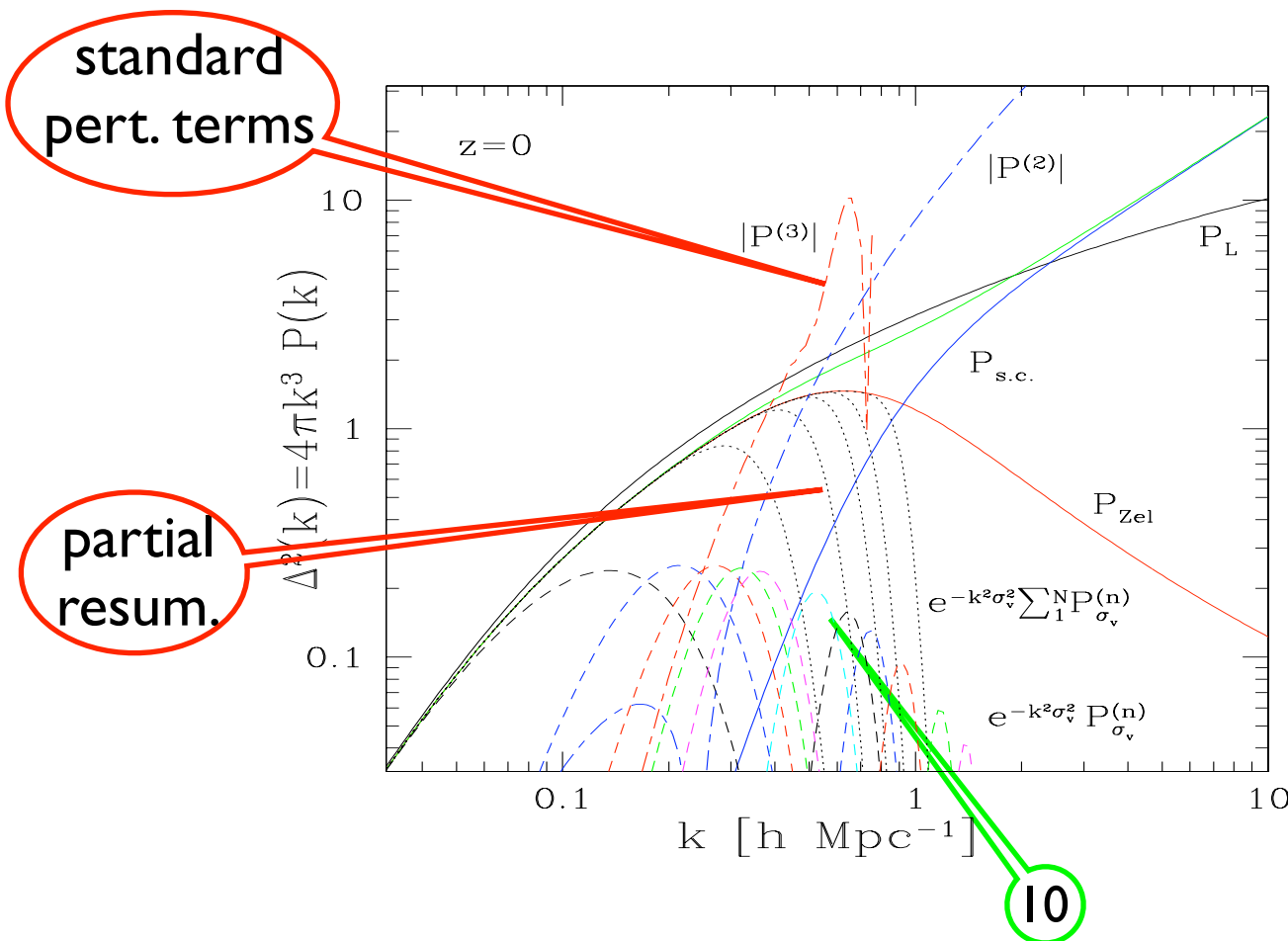
$$\tilde{\delta}(\mathbf{k}, a) = \sum_{n=1}^{\infty} \int d\mathbf{k}_1..d\mathbf{k}_n \delta_D(\mathbf{k}_1 + .. + \mathbf{k}_n - \mathbf{k}) F_n^s(\mathbf{k}_1, .., \mathbf{k}_n; a) \tilde{\delta}_{L0}(\mathbf{k}_1)..\tilde{\delta}_{L0}(\mathbf{k}_n)$$

If $\epsilon(k, a)$ depends on wavenumber the time-dependence of F_n^s does **not** factor out.

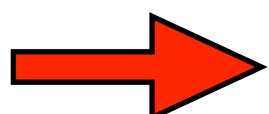
$$P(k) = \langle \delta \delta \rangle = \langle \delta^{(1)} \delta^{(1)} \rangle + \langle \delta^{(3)} \delta^{(1)} \rangle + \langle \delta^{(1)} \delta^{(3)} \rangle + \langle \delta^{(2)} \delta^{(2)} \rangle + ...$$

Test on the Zeldovich Dynamics

(particles moving on straight lines according to their initial velocity)



- standard perturbation theory is **not well-behaved**
- **many orders are relevant** before the nonperturbative term (shell crossing) dominates



Need for improved (resummation) schemes

Sticky model

This model is **identical to the Zeldovich dynamics before shell-crossing**, and only differs afterwards:

Particle pairs do not cross along their longitudinal axis.

For $\mathbf{q} = |\mathbf{q}| \mathbf{e}_1$: $\Delta x_1 = \max(\Delta x_{L1}, 0), \quad \Delta x_2 = \Delta x_{L2}, \quad \Delta x_3 = \Delta x_{L3}$

Then, the power spectrum is equal to the Zeldovich power spectrum + a **nonperturbative correction** associated with the dynamics beyond shell-crossing:

$$P_{\text{sticky}}(k) = P_{\text{Zel}}(k) + P_{\text{s.c.}}(k)$$

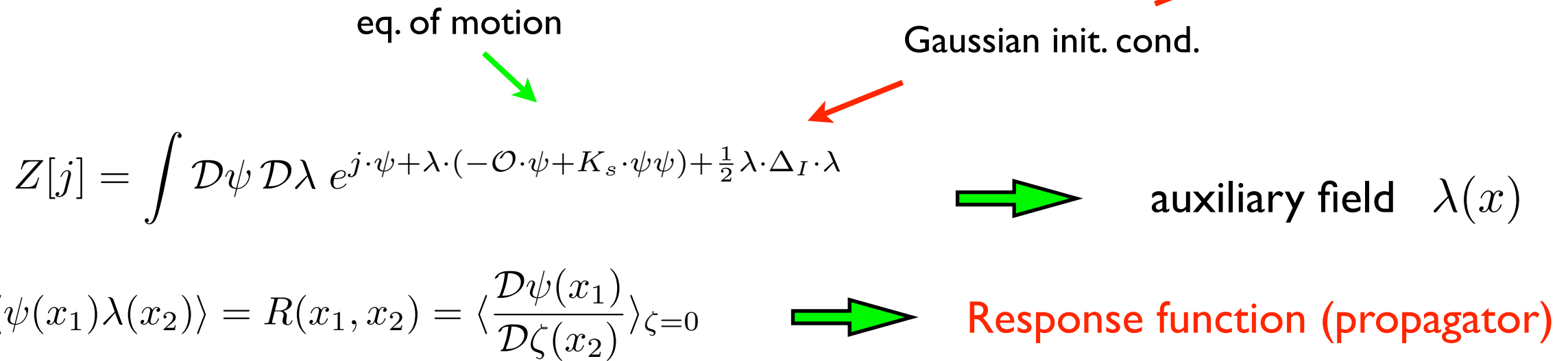
$$P_{\text{s.c.}}(k) = \frac{1}{2} \int \frac{d\mathbf{q}}{(2\pi)^3} e^{-k^2(1-\mu^2)[\sigma_v^2 - I_0(q) - I_2(q)]} e^{-q^2/(2\sigma_{\parallel}^2(q))} \left\{ w\left(\frac{iq}{\sqrt{2}\sigma_{\parallel}(q)}\right) - w\left(\frac{iq - k\mu\sigma_{\parallel}^2(q)}{\sqrt{2}\sigma_{\parallel}(q)}\right) \right\}$$

B- Path-integral formulation

I) Generating functional of many-body correlations

$$\psi(\mathbf{k}, \tau) = \begin{pmatrix} \tilde{\delta}(\mathbf{k}, \tau) \\ \tilde{\theta}(\mathbf{k}, \tau)/\mathcal{H}f \end{pmatrix}$$

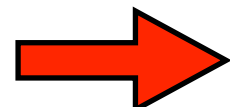
$$Z[j] = \langle e^{j \cdot \psi} \rangle = \int \mathcal{D}\mu_I e^{j \cdot \psi[\mu_I] - \frac{1}{2} \mu_I \cdot \Delta_I^{-1} \cdot \mu_I}$$



It measures the sensitivity to perturbations, or to the initial conditions

Memory of the dynamics

2) Use perturbative schemes to compute $Z[j]$



Power spectrum, bispectrum, ...

I-loop order
(i.e., up to P_L^2)

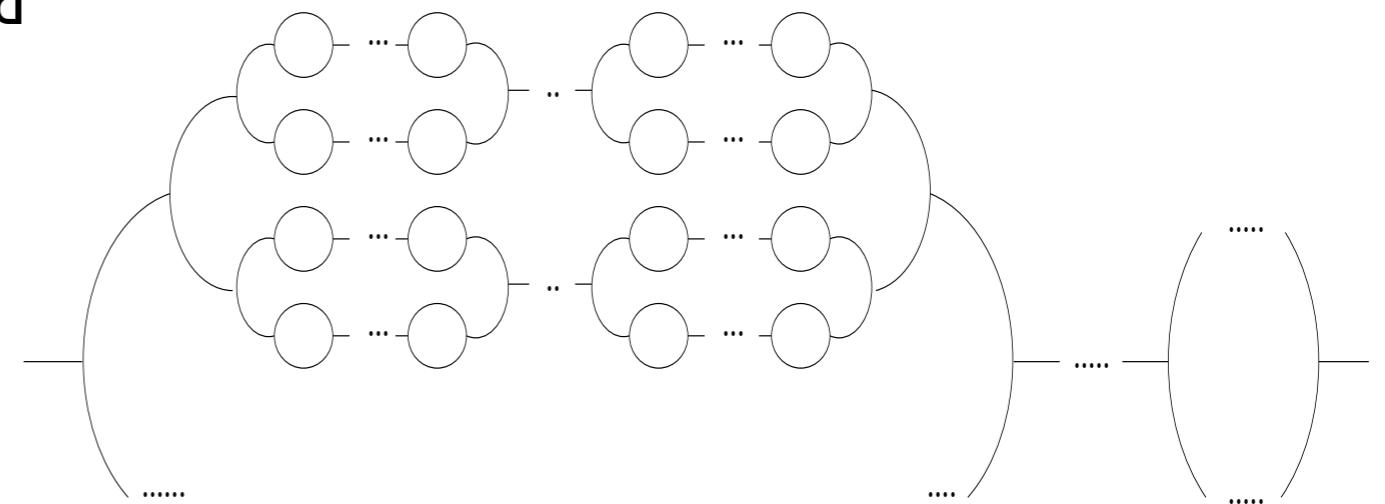
a) Standard perturbation theory

$$P(k) = C_2 = \text{---} + 8 \text{ (a)} + 2 \text{ (b)} + 2 \text{ (c)}$$

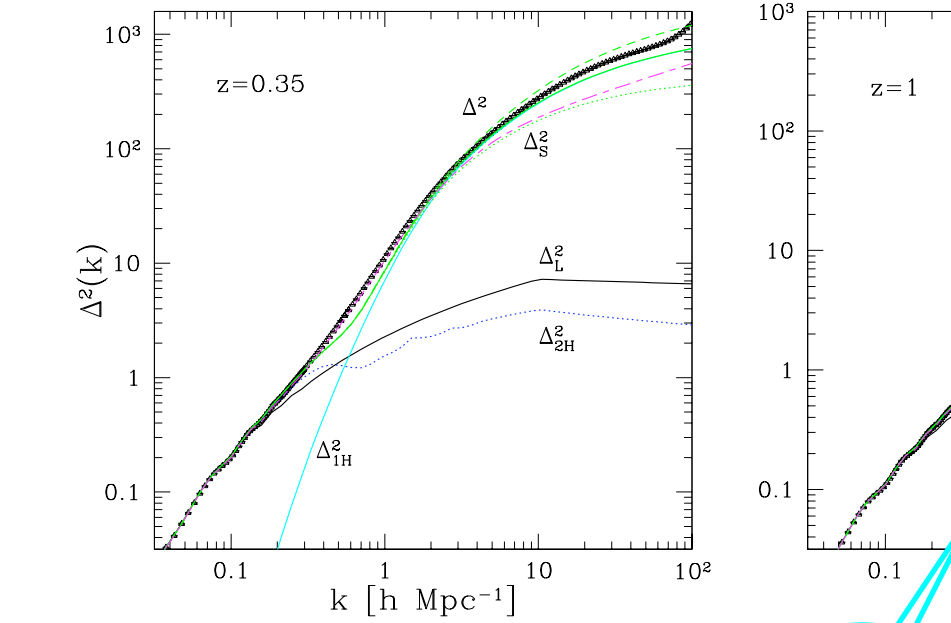
b) Direct steepest-descent method

$$P(k) = \text{---} + C_1 \text{ ---} + 2 \text{ (b)} = \text{---} + \dots + \text{---} + \dots + \text{---} + \dots + \text{---}$$

c) 2PI effective action method

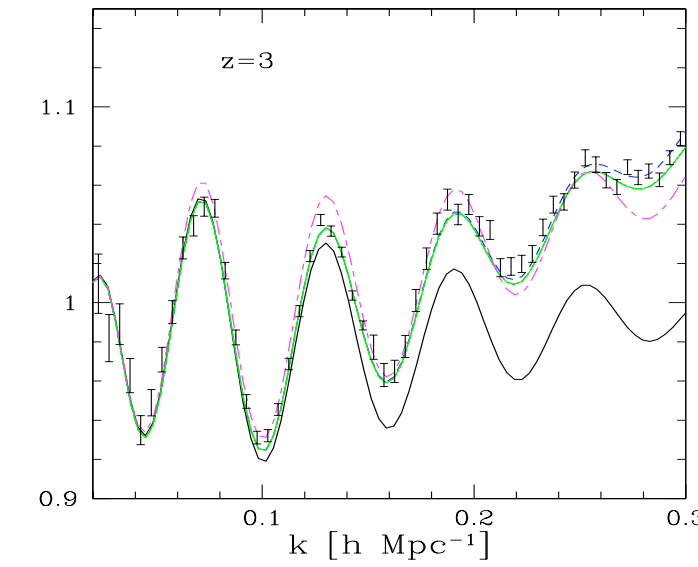
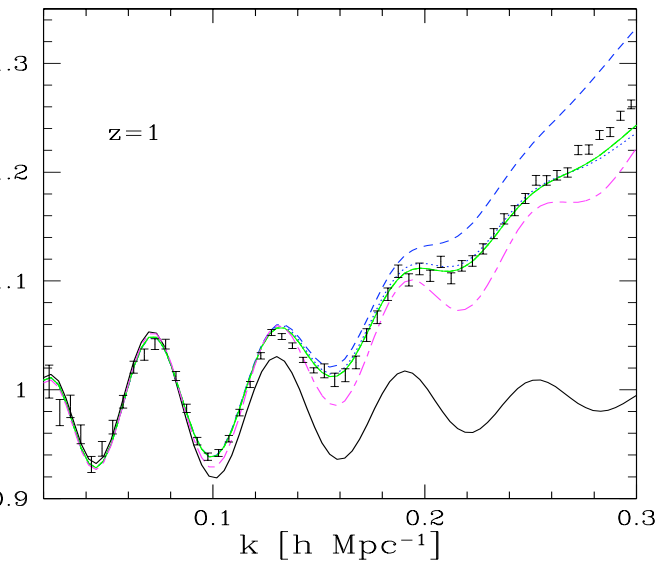
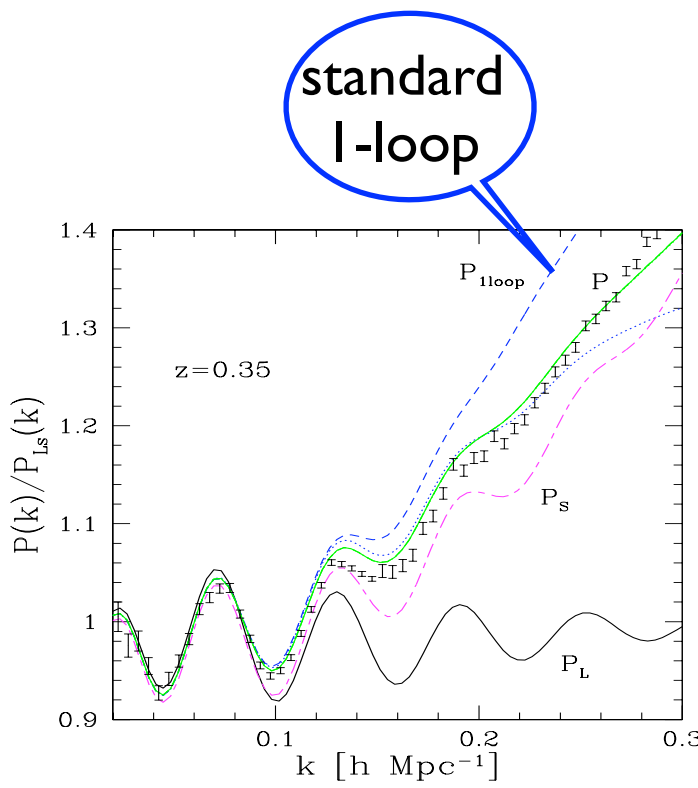
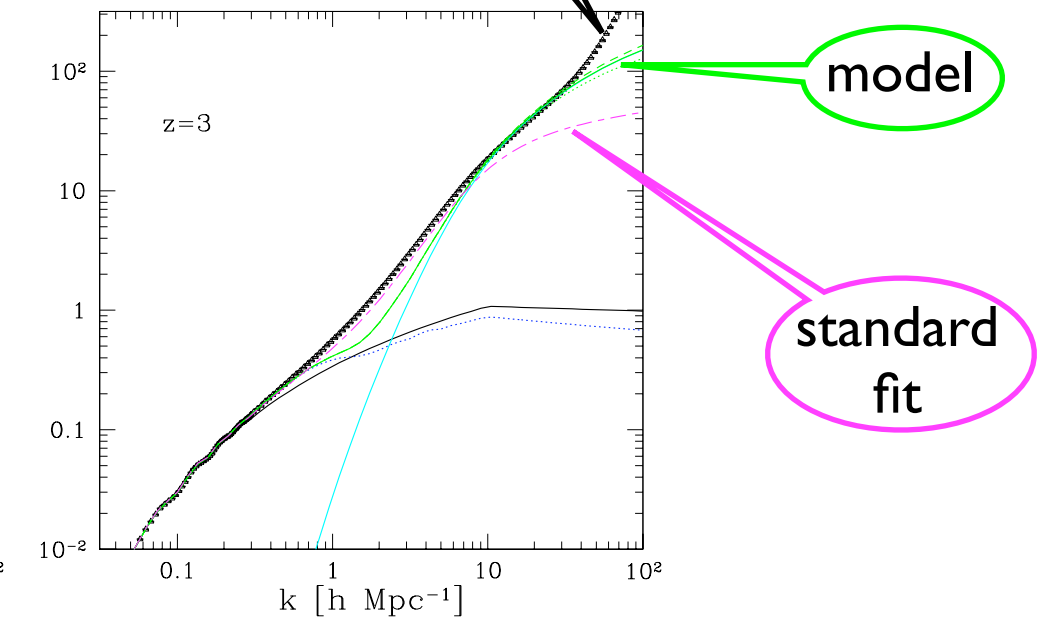
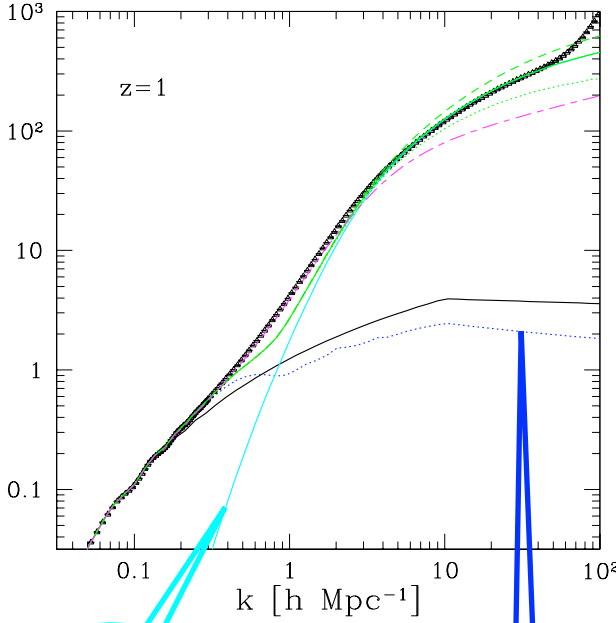


Results for the power spectrum (CDM)

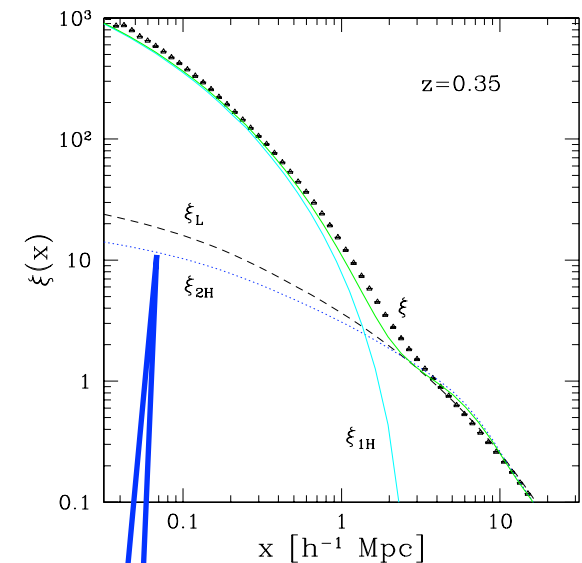


1-halo term

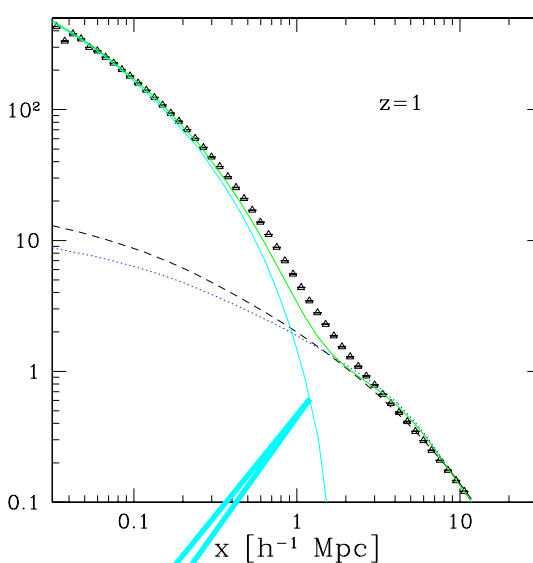
2- halo term



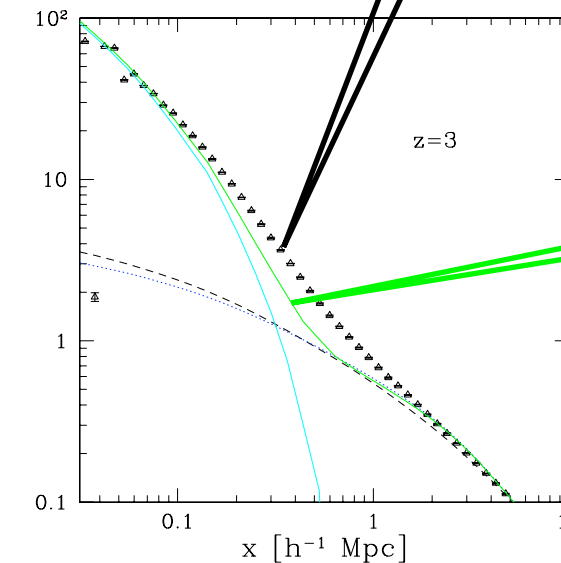
Results for the two-point correlation function (CDM)



2- halo
term

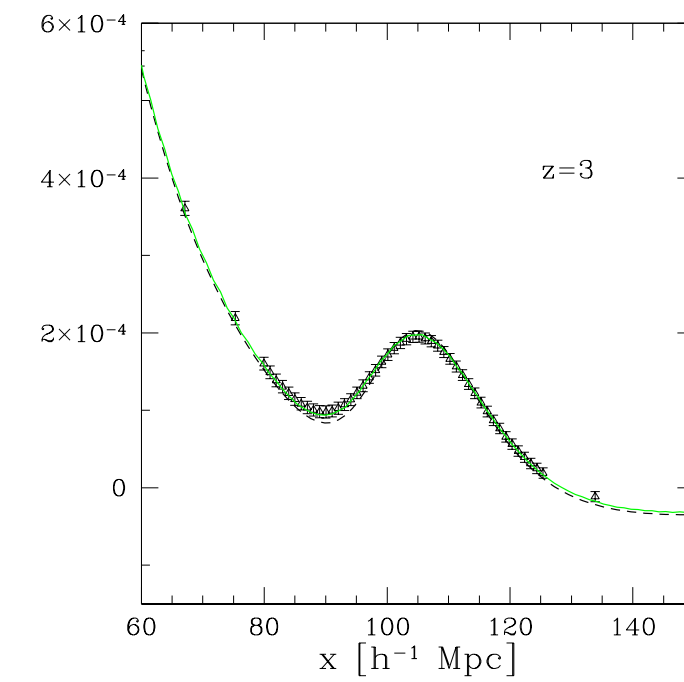
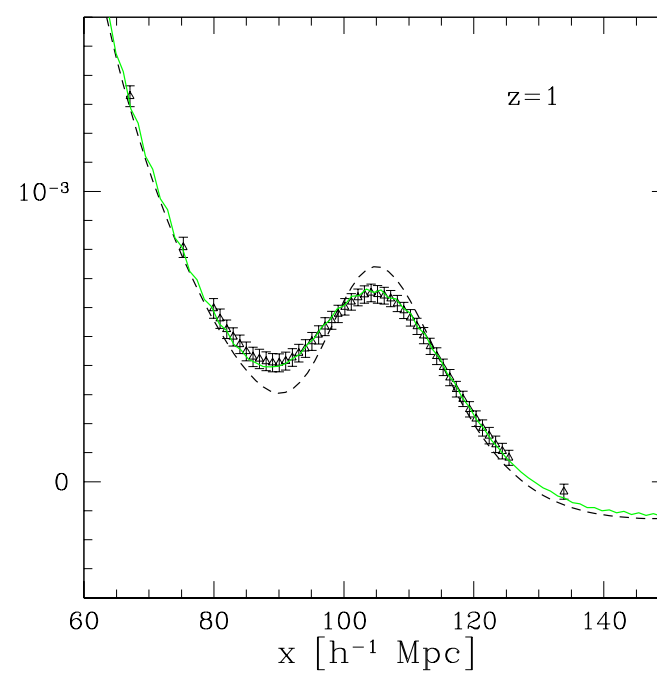
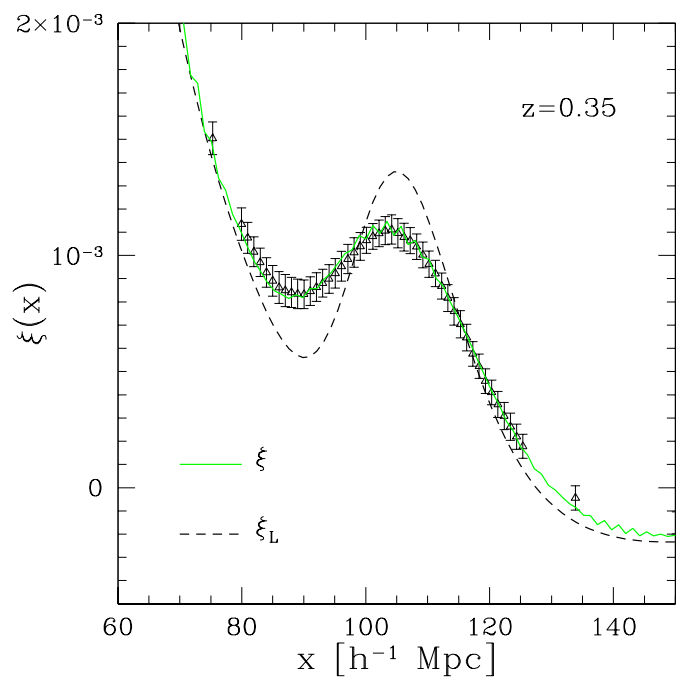


l-halo
term



simulation

model



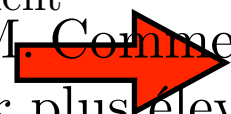
Eulerian / Lagrangian frameworks

A- Eulerian framework: high-k resummation

$$P(k) = \text{Diagram} + \dots \rightarrow \tilde{R}(\mathbf{k}, \tau; \mathbf{k}', \tau_I) = \delta_D(\mathbf{k} - \mathbf{k}') \frac{D}{D_I} e^{-(D-D_I)^2 k^2 \sigma_v^2 / 2}$$

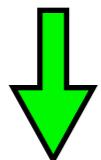
Gaussian decay at late times

Assumption of a wide separation of scales



Linear “effective” equation of motion, with random coefficient, for each \mathbf{k} .

$$\frac{\partial \tilde{\delta}}{\partial \tau}(\mathbf{k}, \tau) = \int d\mathbf{w}_1 d\mathbf{w}_2 \delta_D(\mathbf{w}_1 + \mathbf{w}_2 - \mathbf{k}) (\dots) \tilde{\delta}(\mathbf{w}_1, \tau) \tilde{\delta}(\mathbf{w}_2, \tau)$$



$$\begin{aligned} \frac{\partial \tilde{\delta}}{\partial \tau}(\mathbf{k}, \tau) &= \tilde{\delta}(\mathbf{k}, \tau) \int d\mathbf{w} (\dots) \tilde{\delta}_L(\mathbf{w}, \tau) \\ &= \hat{\alpha}(\mathbf{k}, \tau) \tilde{\delta}(\mathbf{k}, \tau) \end{aligned}$$

$$\hat{\alpha}(\mathbf{k}) = \int d\mathbf{w} \frac{\mathbf{k} \cdot \mathbf{w}}{w^2} \tilde{\delta}_{L0}(\mathbf{w})$$

$$\left\{ \begin{array}{l} \hat{\delta}(\mathbf{k}, D) = D \tilde{\delta}_{L0}(\mathbf{k}) e^{\hat{\alpha}(D-D_I)} \\ \hat{\delta}(\mathbf{x}, D) = D \delta_{L0}[\mathbf{x} - \mathbf{s}_L(\mathbf{q}=0, D), D] \end{array} \right.$$

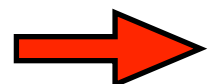
Sweeping effect

B- Lagrangian framework

Trajectories $\mathbf{x}(\mathbf{q}, \tau)$

Divergence of the displacement field

$$\kappa(\mathbf{q}, \tau) = 3 - \frac{\partial \mathbf{x}}{\partial \mathbf{q}}$$



No longer sensitive to the sweeping effect

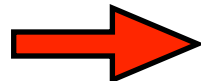
One can apply the same procedure, even without explicit resummation

separation of scale

Linear “effective” equation of motion
with random coefficients

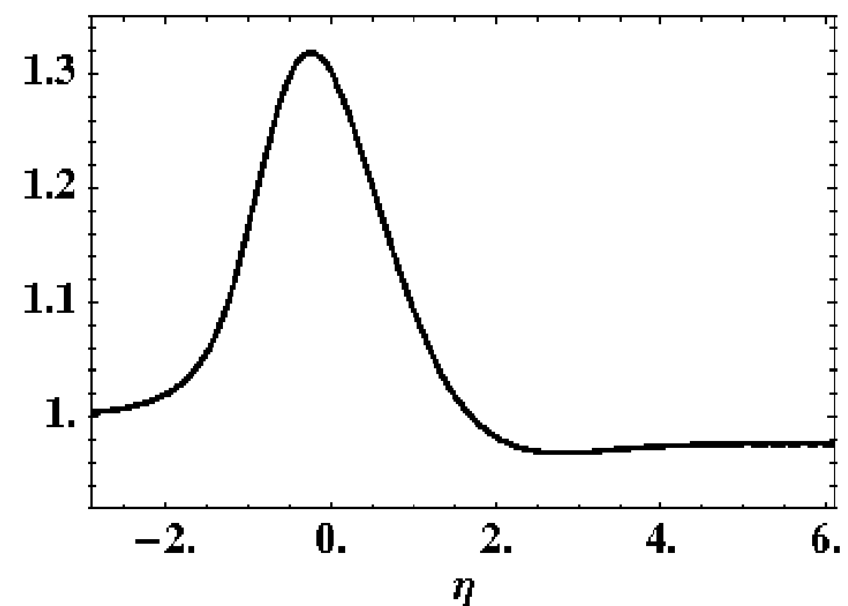
$$\kappa''(\mathbf{k}, \eta) + \frac{1}{2}\kappa'(\mathbf{k}, \eta) - \frac{3}{2}\kappa(\mathbf{k}, \eta) = e^\eta \hat{\alpha}(\mathbf{k}) \left(\kappa''(\mathbf{k}, \eta) + \frac{1}{2}\kappa'(\mathbf{k}, \eta) \right) + e^\eta \hat{\beta}(\mathbf{k}) \left(\omega''(\mathbf{k}, \eta) + \frac{1}{2}\omega'(\mathbf{k}, \eta) \right)$$

$$R(\eta) = \int_{-\infty}^{\infty} \hat{\kappa}(\eta; \hat{\alpha}, \hat{\beta}) \mathcal{P}(\hat{\alpha}, \hat{\beta}) d\hat{\alpha} d\hat{\beta}$$



No Gaussian decay at late times

$$\hat{R}(\eta)$$



Exact results for toy models: adhesion model

Work on firm grounds: beyond perturbative approaches
and partial resummations

Include some nonperturbative shell-crossing phenomena

Complete and consistent picture for similar dynamics

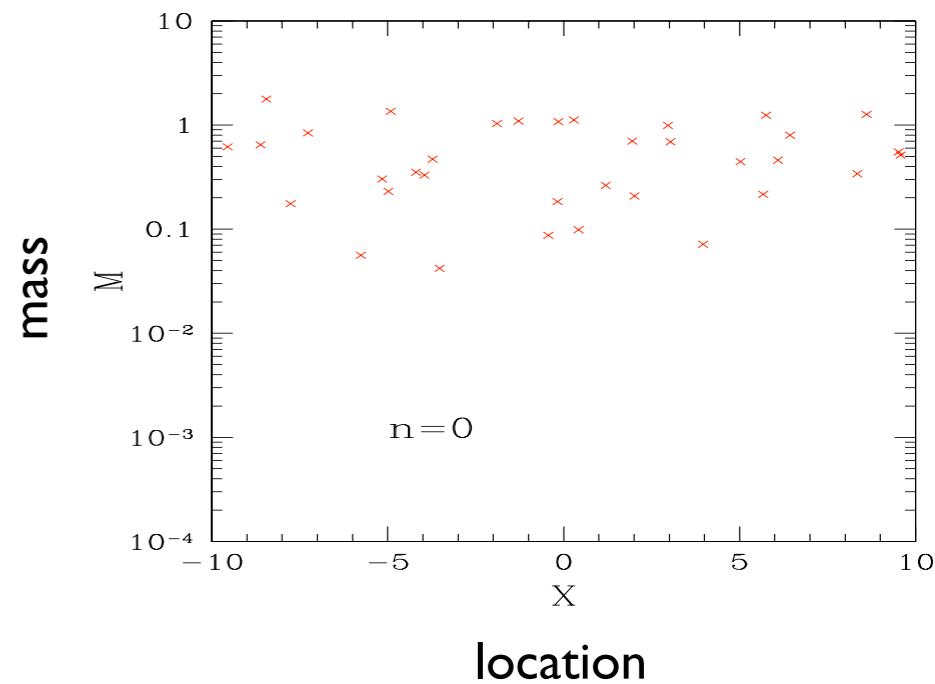
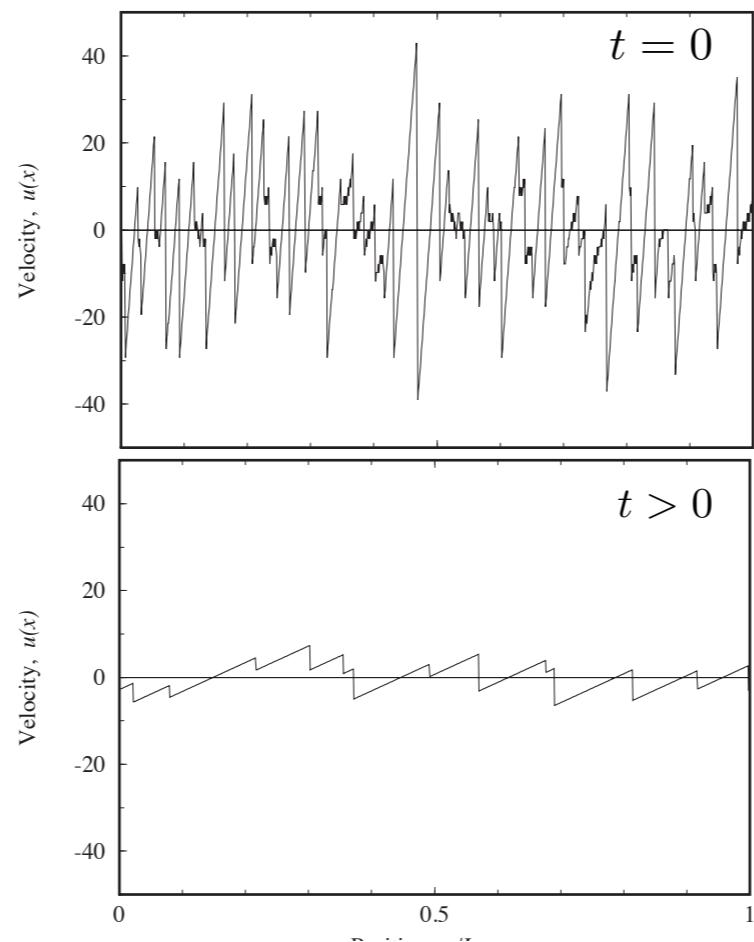
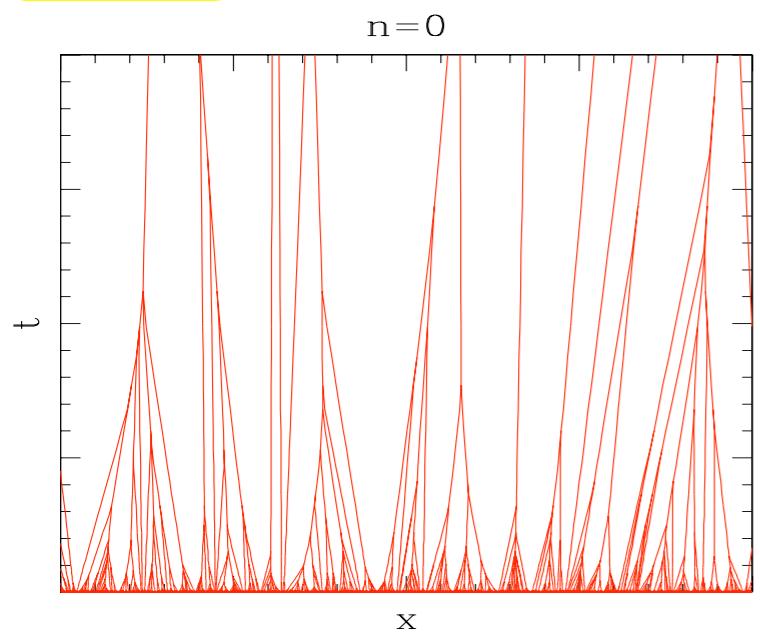
Deeper understanding of some processes

Benchmark for approximation schemes

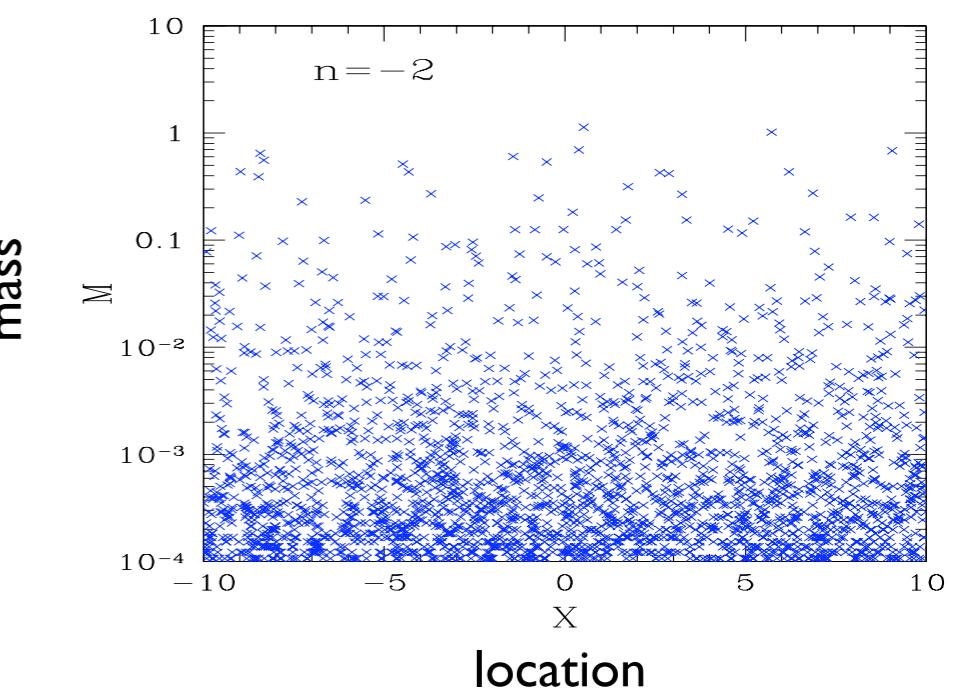
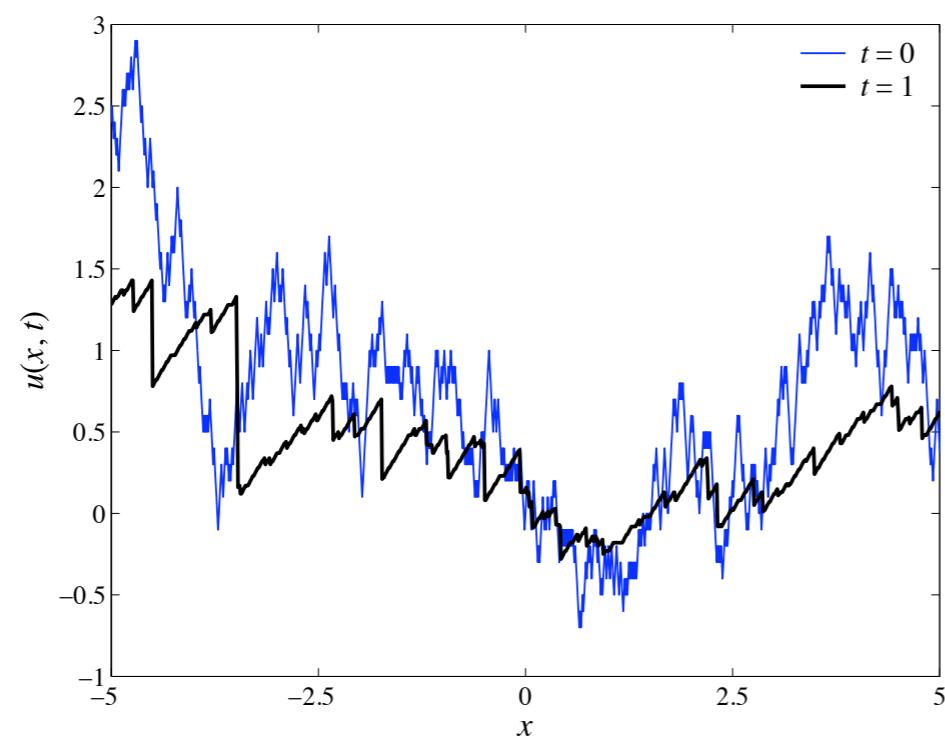
F. Bernardeau & P.V., 2010a,b - P.V., 2009a,b,c - P.V. & F. Bernardeau, 2010

S. N. Gurbatov, A. I. Saichev, S. F. Shandarin, 1989 - S. F. Shandarin 2010 -
M. Vergassola, B. Dubrulle, U. Frisch, A. Noullez, 1994 - D. H. Weinberg & J. E. Gunn, 1990

$n = 0 :$

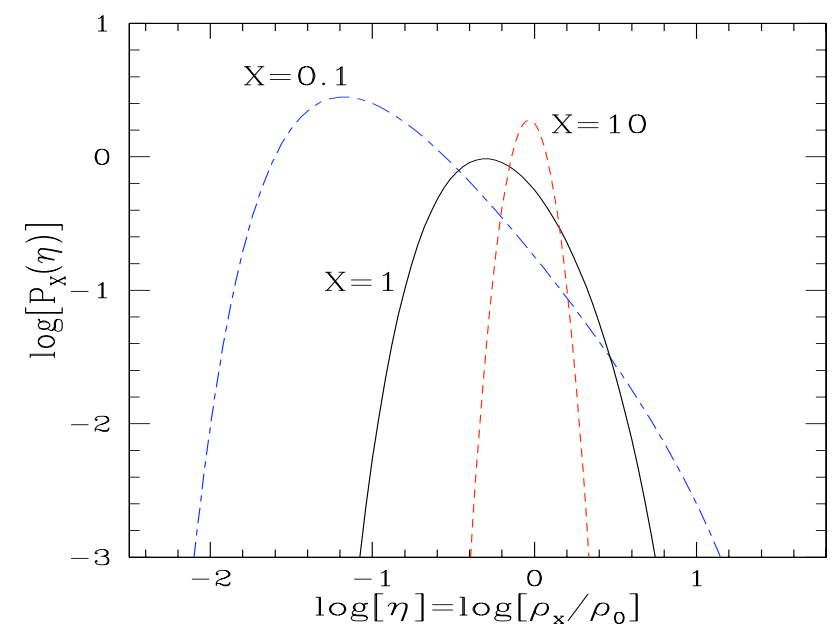
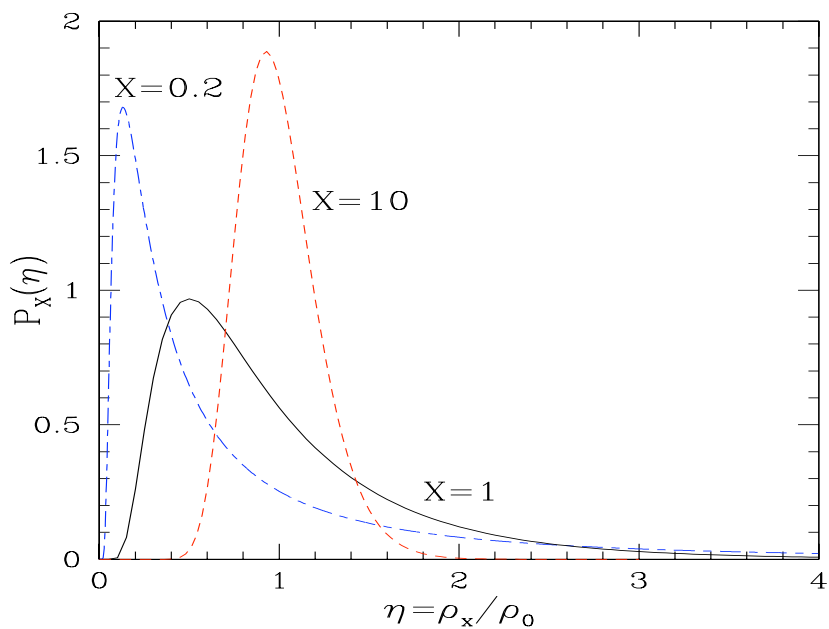


$n = -2 :$



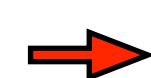
A- Brownian initial velocity, n=-2 (in 1D)

Probability distribution
of the density contrast



$$\eta = \frac{m}{\bar{\rho} x}, \quad \eta \geq 0 : \quad \mathcal{P}_X(\eta) = \sqrt{\frac{X}{\eta}} \eta^{-3/2} e^{-X(\sqrt{\eta}-1/\sqrt{\eta})^2}$$

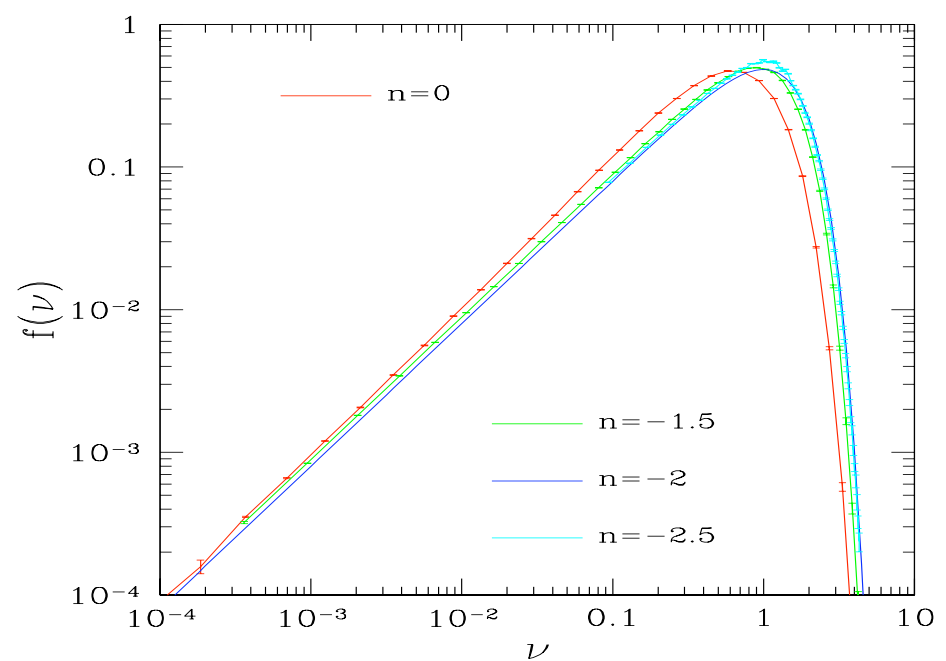
$$S_n = \frac{\langle \eta^n \rangle_c}{\langle \eta^2 \rangle_c^{n-1}} = (2n-3)!!$$



exact realization of the
stable clustering ansatz

Cluster mass function: $N(M) = \frac{1}{\sqrt{\pi}} M^{-3/2} e^{-M}$

exact realization of the
Press & Schechter ansatz



B- Response functions (propagators)

I) Eulerian framework

$$R^\delta(x, t; q_0) = \left\langle \frac{\mathcal{D}\delta(x, t)}{\mathcal{D}\delta_{L0}(q_0)} \right\rangle$$

$$R^\delta(x, t; q_0) = p_x(u, t)$$

$$\text{with } u = \frac{x - q_0}{t}$$

The Eulerian response function is set by the 1-point probability distribution of the velocity.

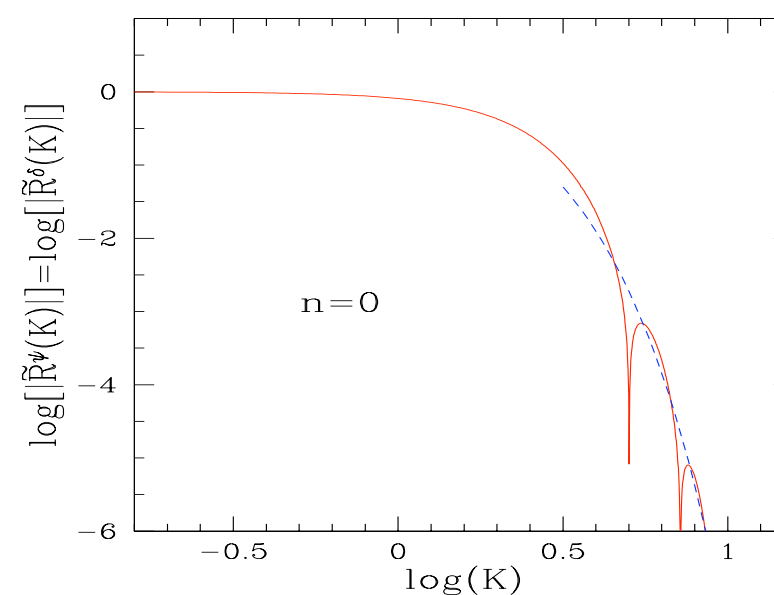
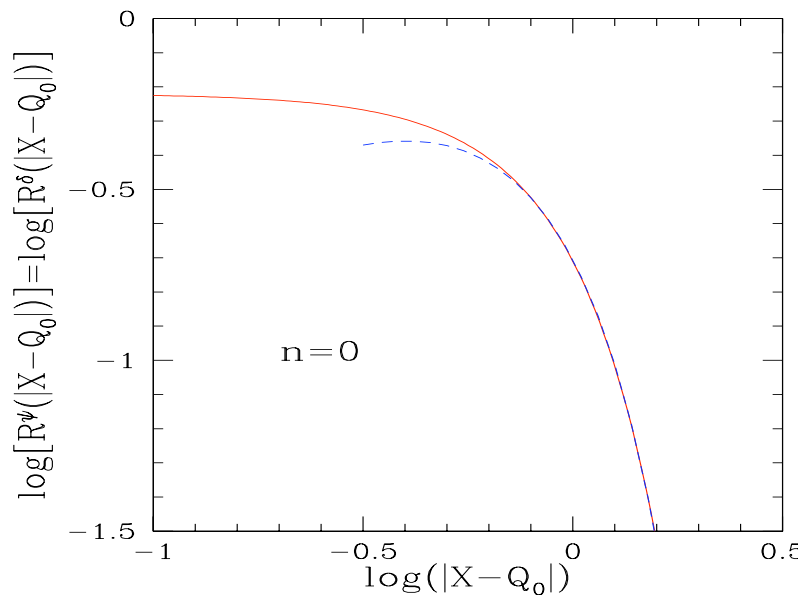
Linear regime (long wavelengths):

$$R_L^\delta(x, t; q_0) = \frac{1}{\sqrt{2\pi} \sigma_{u_0}(x)} e^{-(x-q_0)^2/(2t^2\sigma_{u_0}^2(x))}$$

$$\tilde{R}_L^\delta(k, t) = t e^{-t^2 k^2 \sigma_{u_0}^2 / 2}$$



Gaussian decay

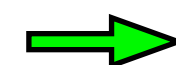


$$n = 0 :$$

$$K \gg 1 : \quad \tilde{R}^\delta(K) \sim K^{1/4} e^{-\frac{\sqrt{2}}{3} K^{3/2} - \frac{\omega_1}{\sqrt{2}} \sqrt{K}}$$

$$\times \cos \left[\frac{\sqrt{2}}{3} K^{3/2} - \frac{\omega_1}{\sqrt{2}} \sqrt{K} + \frac{\pi}{8} \right]$$

$$-1 < n < 1, \quad |x - q_0| \rightarrow \infty : \quad R^\delta(x, t; q_0) \sim e^{-|x - q_0|^{n+3}/t^2}$$



n-dependent behavior

2) Lagrangian framework

$$\kappa(q, t) = 1 - \frac{\partial x}{\partial q}$$

$$\rho(x, t) = \frac{\rho_0}{1 - \kappa(q, t)}$$

$$R^\kappa(q, t; q_0) = \langle \frac{\mathcal{D}\kappa(q, t)}{\mathcal{D}\kappa_{L0}(q_0)} \rangle$$

Using the geometric construction, one obtains

$$R^\kappa(q, t; q_0) = t \int_{\rho_0 |q - q_0|}^{\infty} dm n(m, t) \left(1 - \frac{|q - q_0|}{m/\rho_0}\right)$$

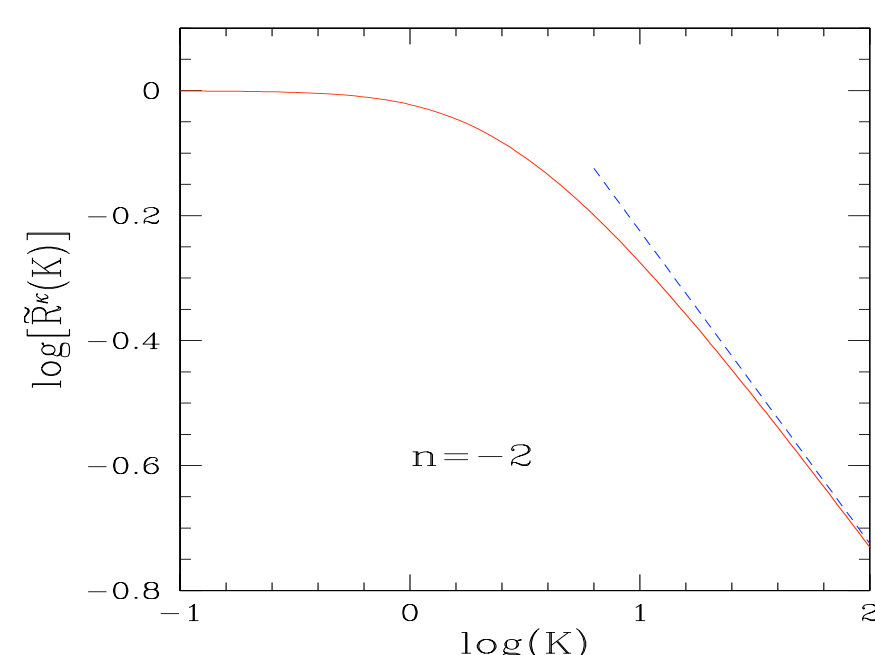
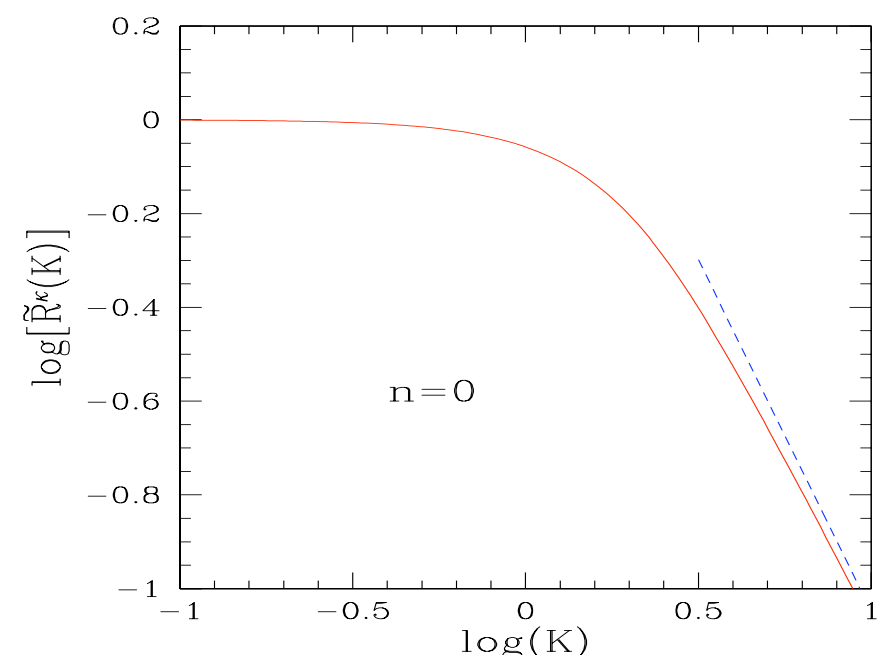
$$\tilde{R}^\kappa(k, t) = 2t \int_0^{\infty} dm n(m, t) \frac{1 - \cos(km/\rho_0)}{k^2 m/\rho_0}$$

The **Lagrangian response** function is set by the cluster **mass function**.

$$\frac{|q - q_0|}{L(t)} \gg 1 : R^\kappa(q, t; q_0) \sim e^{-|q - q_0|^{n+3}/t^2}$$

$$k \gg L(t)^{-1} : \quad \tilde{R}^\kappa(k, t) \sim k^{-(n+3)/2}$$

n-dependent power-law decay



Combined models

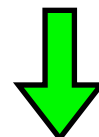
For some observational probes that are sensitive to both quasilinear and nonlinear regimes (e.g., weak lensing), it is necessary to simultaneously describe both large and small scales.

Combine
the accuracy and systematic character of **perturbative approaches** on large scales
with
the reasonable description of **phenomenological models** on small scales

As in the halo model (but from a Lagrangian point of view), decompose the power spectrum as

$$P(k) = P_{2H}(k) + P_{1H}(k)$$

“2-halo term”



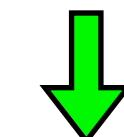
perturbative contribution

$$P_{2H}(k) \simeq F_{2H}(1/k) P_{\text{pert}}(k)$$

high-k behavior solved by going beyond standard perturbation theory

resummation schemes

“1-halo term”



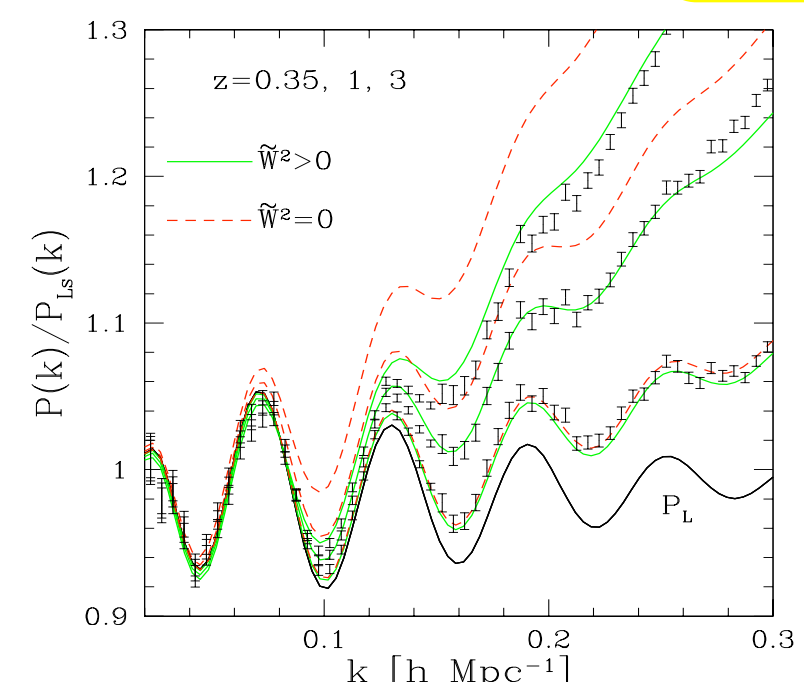
nonperturbative contribution

$$P_{1H}(k) = \int_0^\infty \frac{d\nu}{\nu} f(\nu) \frac{M}{\bar{\rho}(2\pi)^3} \left(\tilde{u}_M(k)^2 - \tilde{W}(k q_M)^2 \right)$$

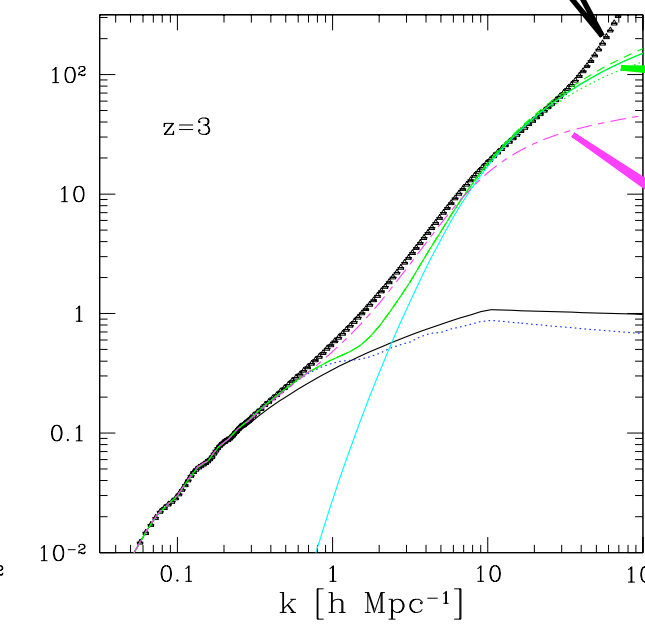
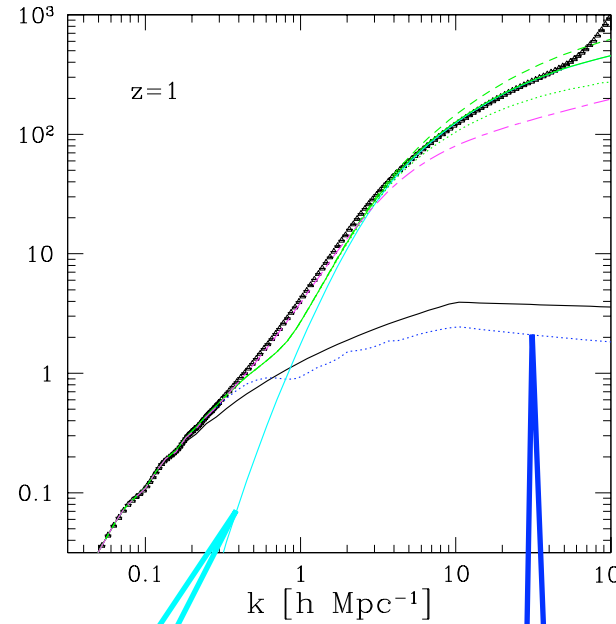
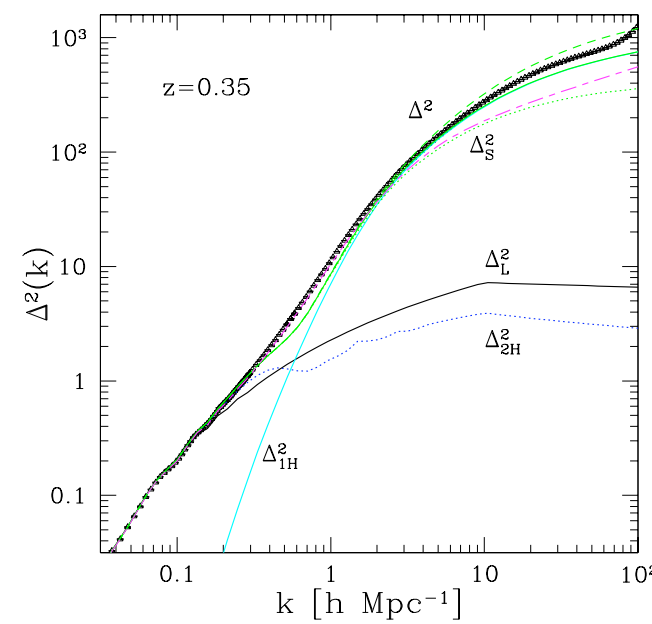
halo mass function

halo density profile

low-k behavior solved by counterterm



Results for the power spectrum



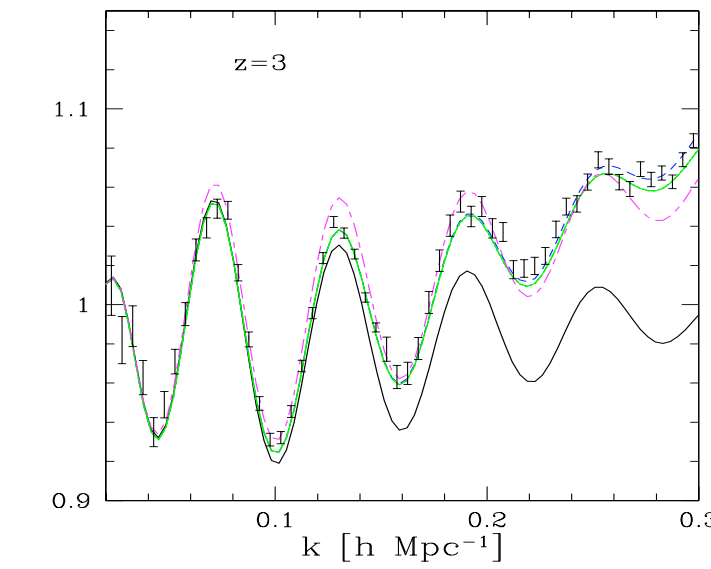
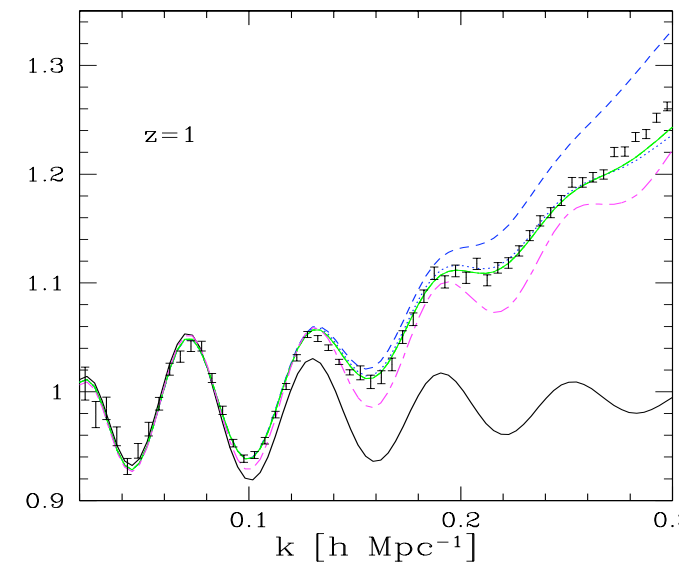
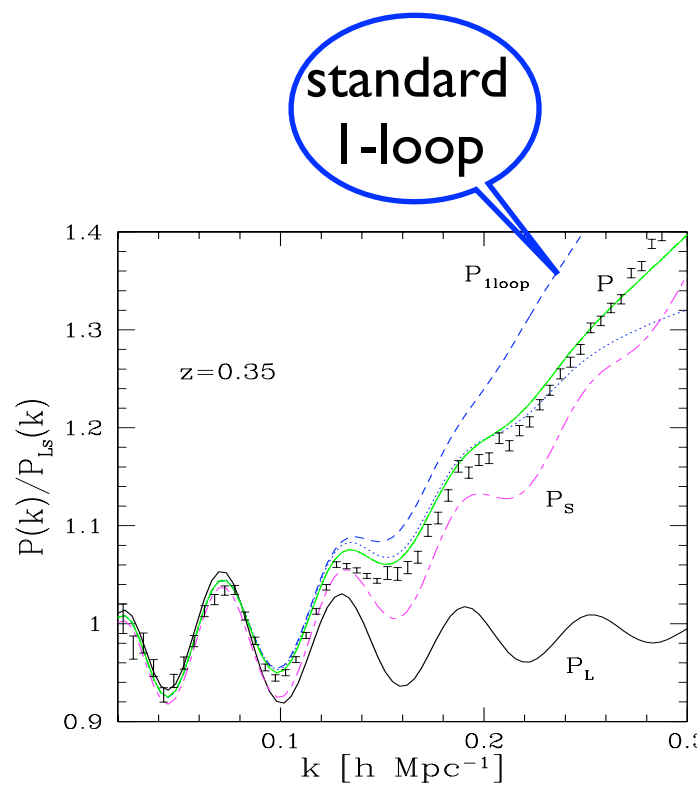
1-halo term

2- halo term

simulation

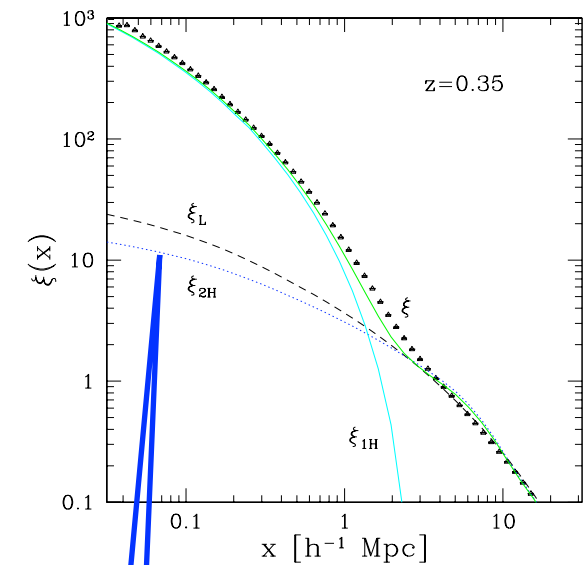
model

standard fit

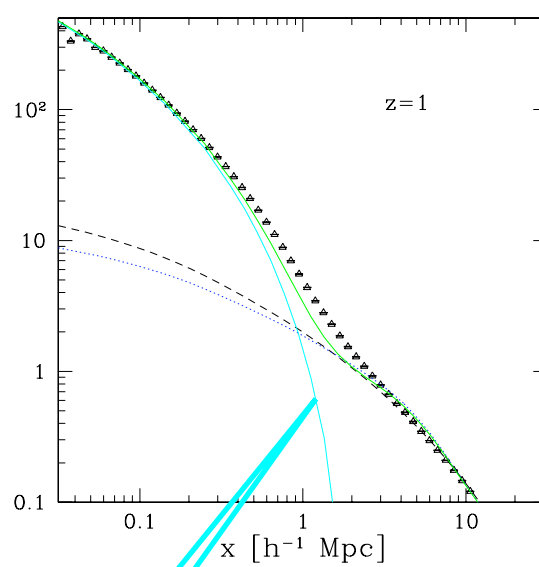


standard I-loop

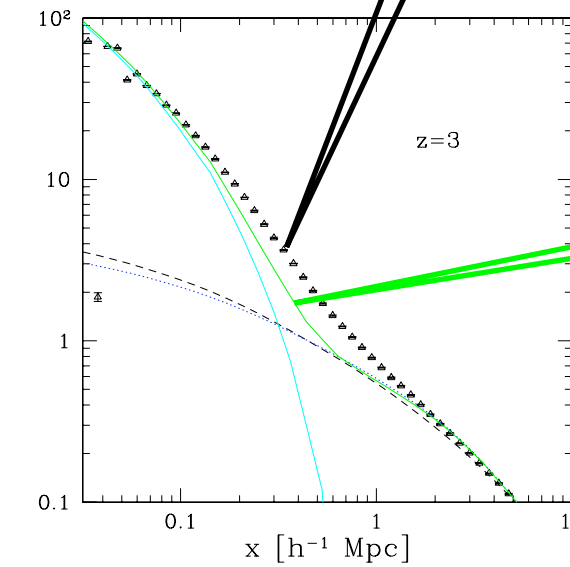
Results for the two-point correlation function



2- halo
term

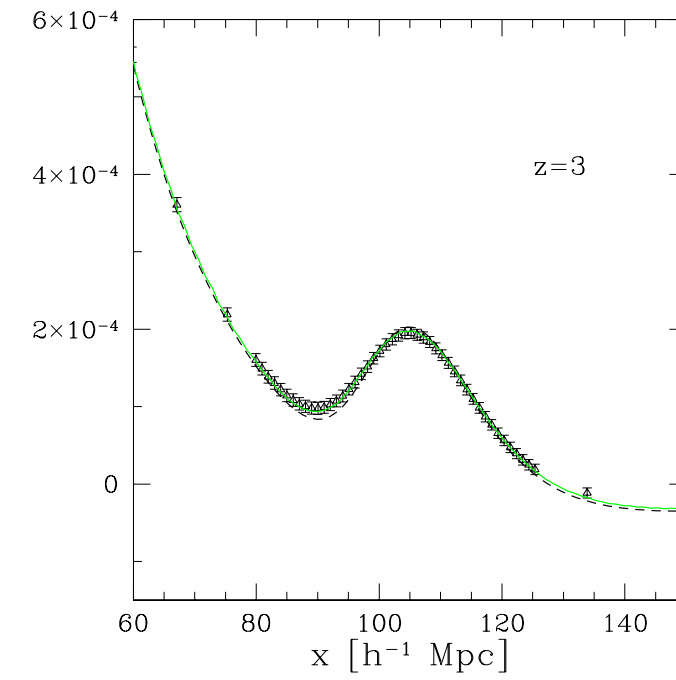
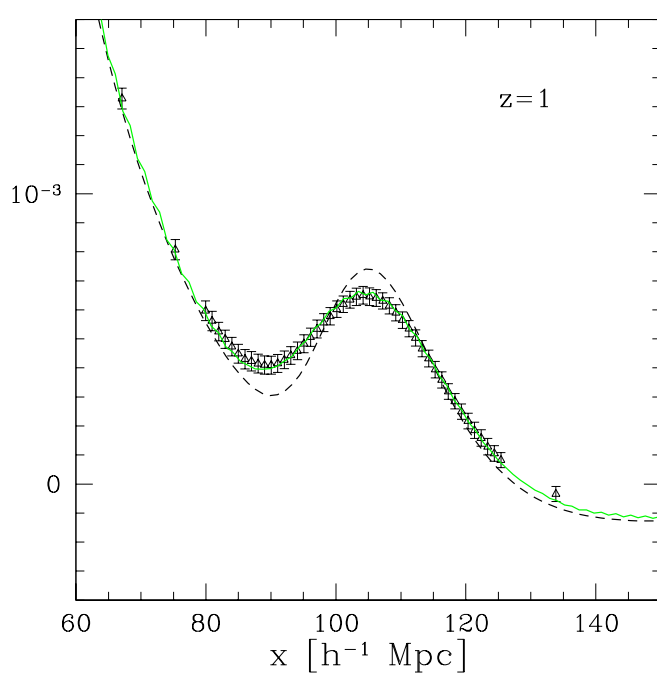
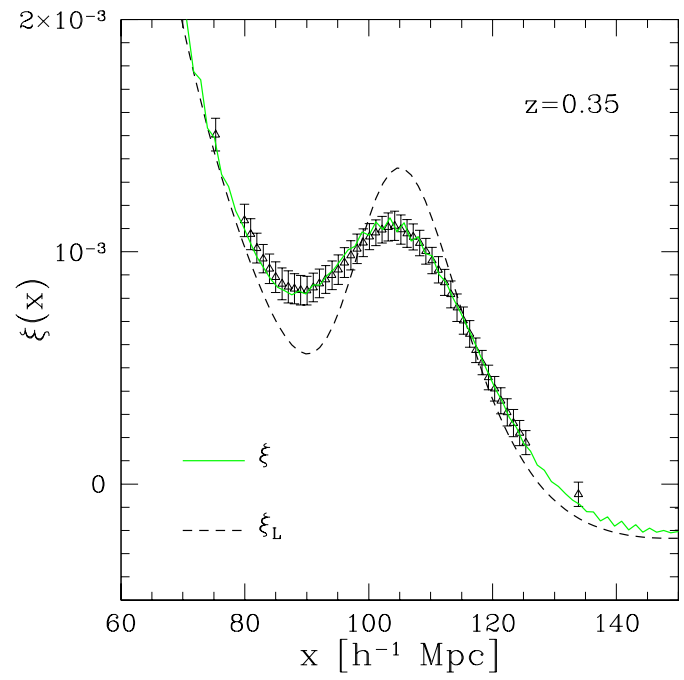


1-halo
term



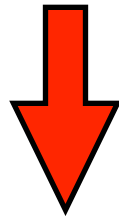
simulation

model



B- Bispectrum

In order to **break degeneracies**, it is useful to consider higher-order statistics beyond the power spectrum (i.e., 2-pt correlation).



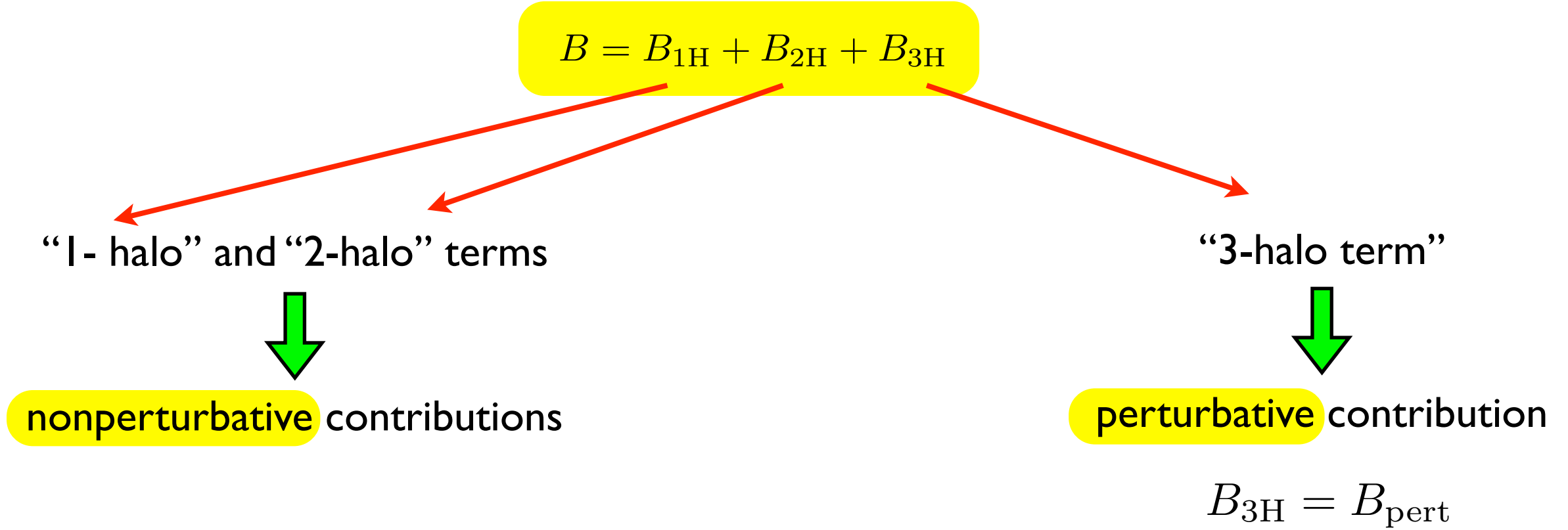
3-pt correlation / bispectrum

This is also useful to constrain **primordial non-Gaussianities**

I-Method

$$\langle \tilde{\delta}(\mathbf{k}_1) \tilde{\delta}(\mathbf{k}_2) \tilde{\delta}(\mathbf{k}_3) \rangle = \delta_D(\mathbf{k}_1 + \mathbf{k}_2 + \mathbf{k}_3) B(k_1, k_2, k_3)$$

Again, as in the halo model (but from a Lagrangian point of view), we decompose the bispectrum as



$$B_{1H} = \int \frac{d\nu}{\nu} f(\nu) \left(\frac{M}{\bar{\rho}(2\pi)^3} \right)^2 \prod_{j=1}^3 \left(\tilde{u}_M(k_j) - \tilde{W}(k_j q_M) \right)$$

$$B_{2H} = P_L(k_1) \int \frac{d\nu}{\nu} f(\nu) \frac{M}{\bar{\rho}(2\pi)^3} \prod_{j=2}^3 \left(\tilde{u}_M(k_j) - \tilde{W}(k_j q_M) \right) + 2 \text{ cyc.}$$

counterterms

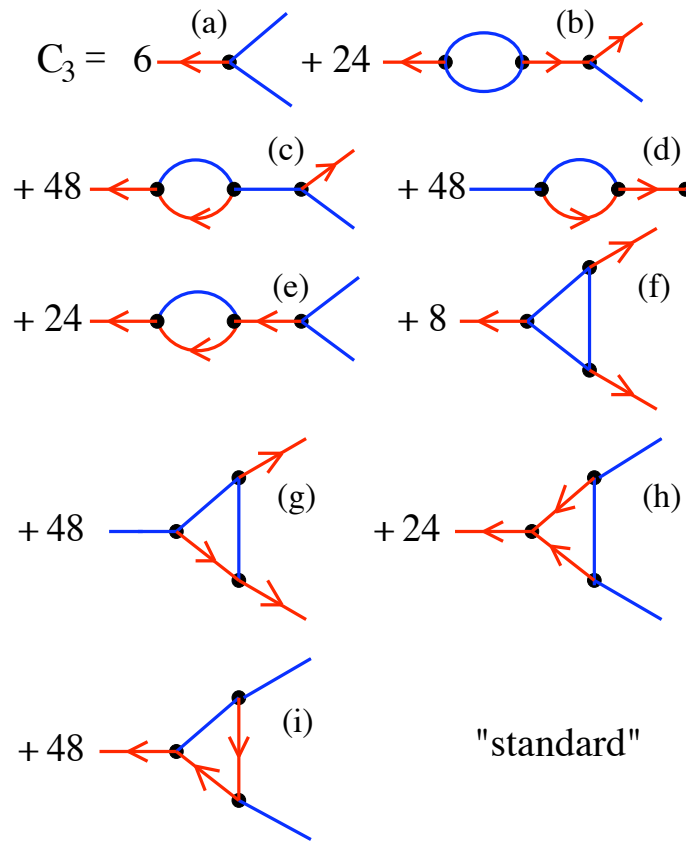
$$B_{1H} \propto k_j^2 \text{ for } k_j \rightarrow 0$$

$$\lambda \rightarrow 0 : B_{1H}(\lambda k_1, \lambda k_2, \lambda k_3) \propto \lambda^6$$

$$B_{2H} \propto P_L(k_j) \text{ for } k_j \rightarrow 0$$

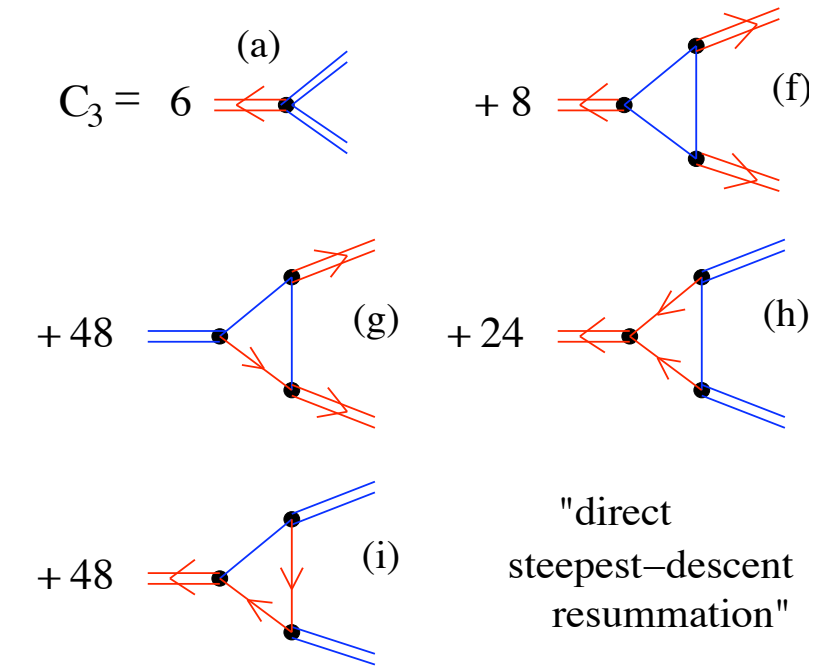
$$\lambda \rightarrow 0 : B_{2H}(\lambda k_1, \lambda k_2, \lambda k_3) \propto \lambda^4 P_L(k)$$

The 3-halo term can be computed from any perturbative scheme



standard perturbation theory

- well-known diagrams
- simpler expressions (time integrals)
- standard 1-loop expression is now well-behaved at high k .



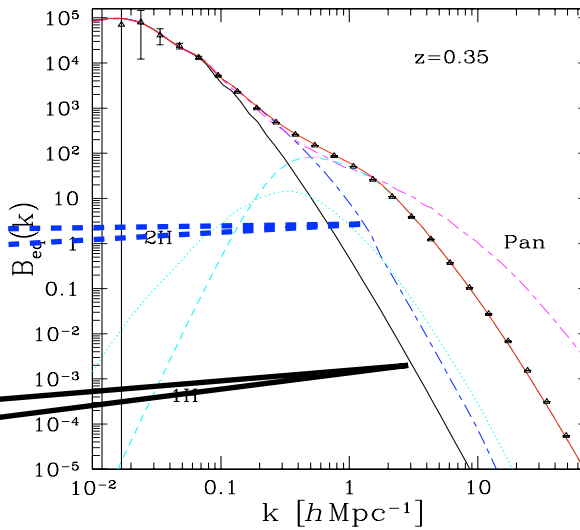
resummation scheme

- fewer but more complex diagrams
- numerical integrations over time

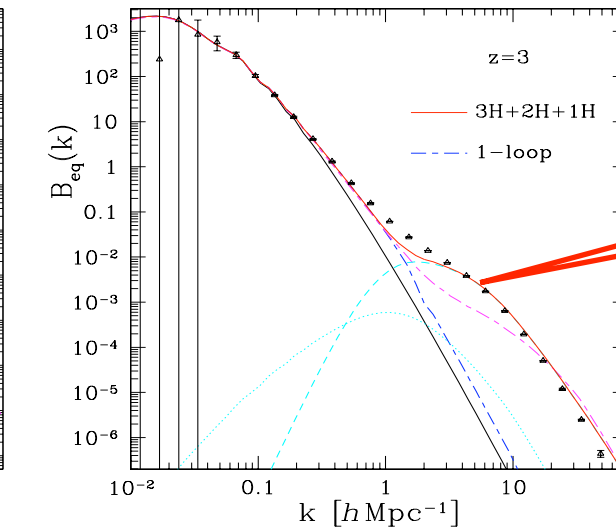
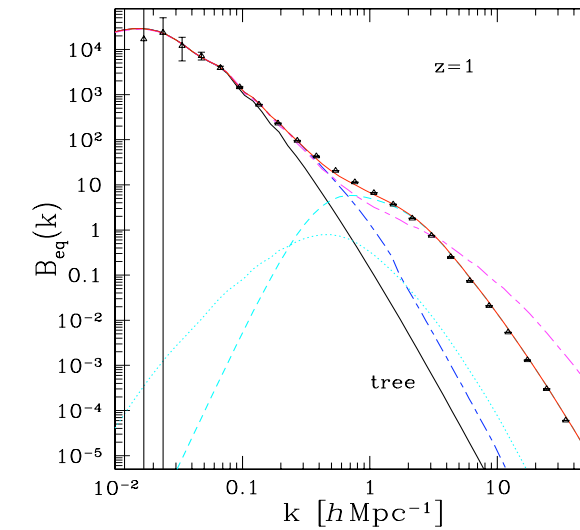
II-Results

standard
1-loop

tree-order

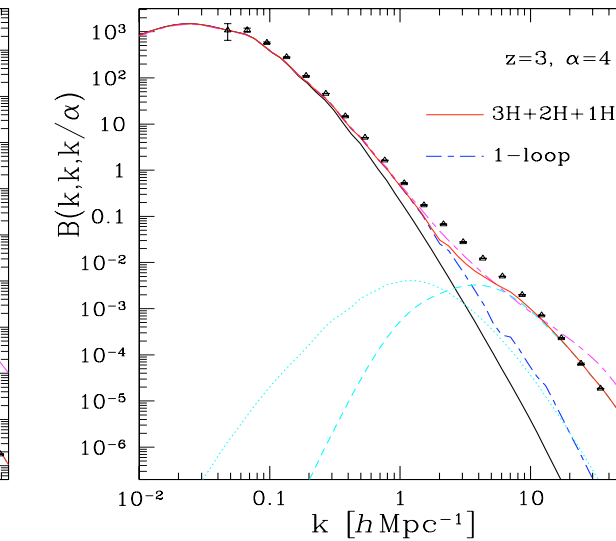
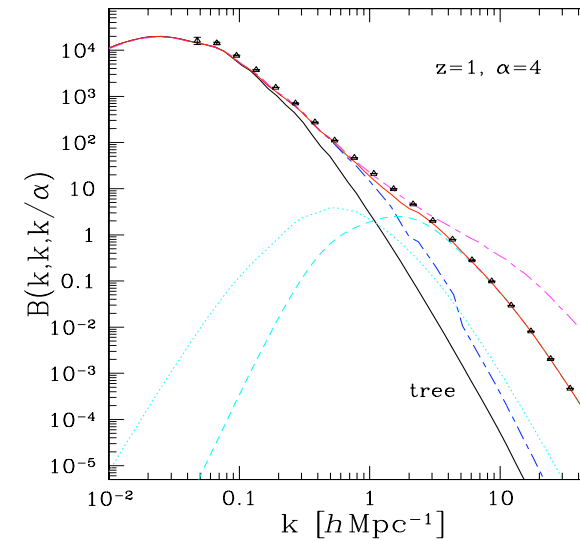
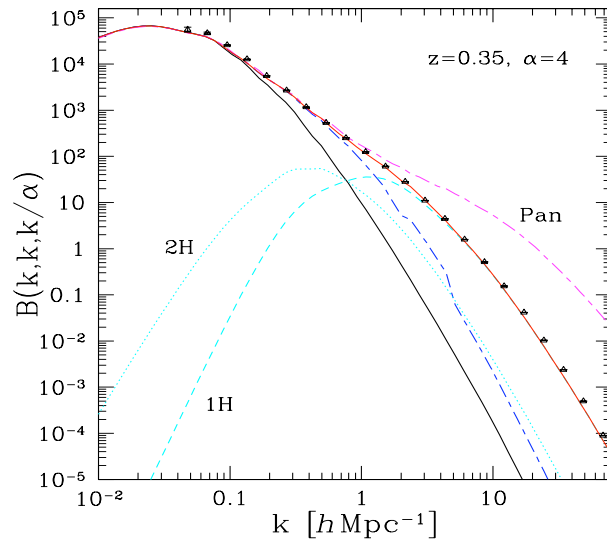


Equilateral triangles

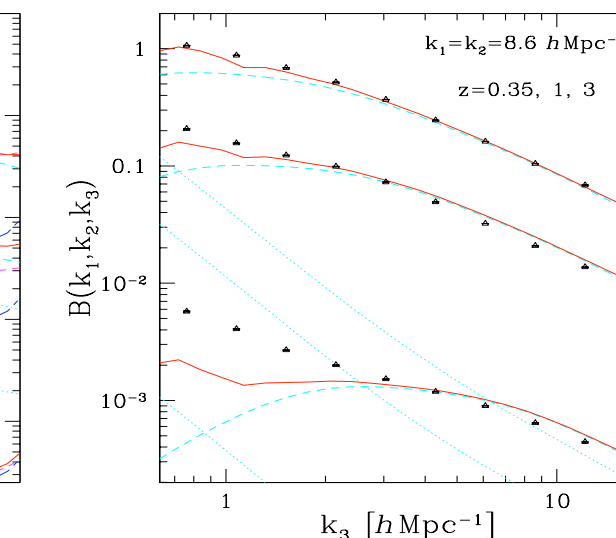
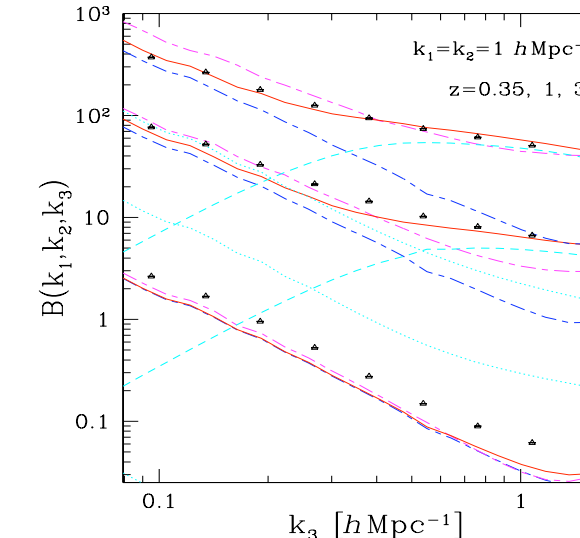
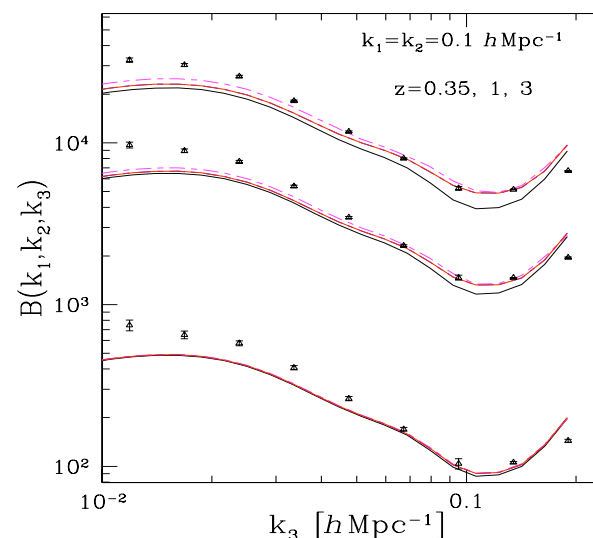


1H+2H+3H

Isosceles triangles at fixed length ratio = 4

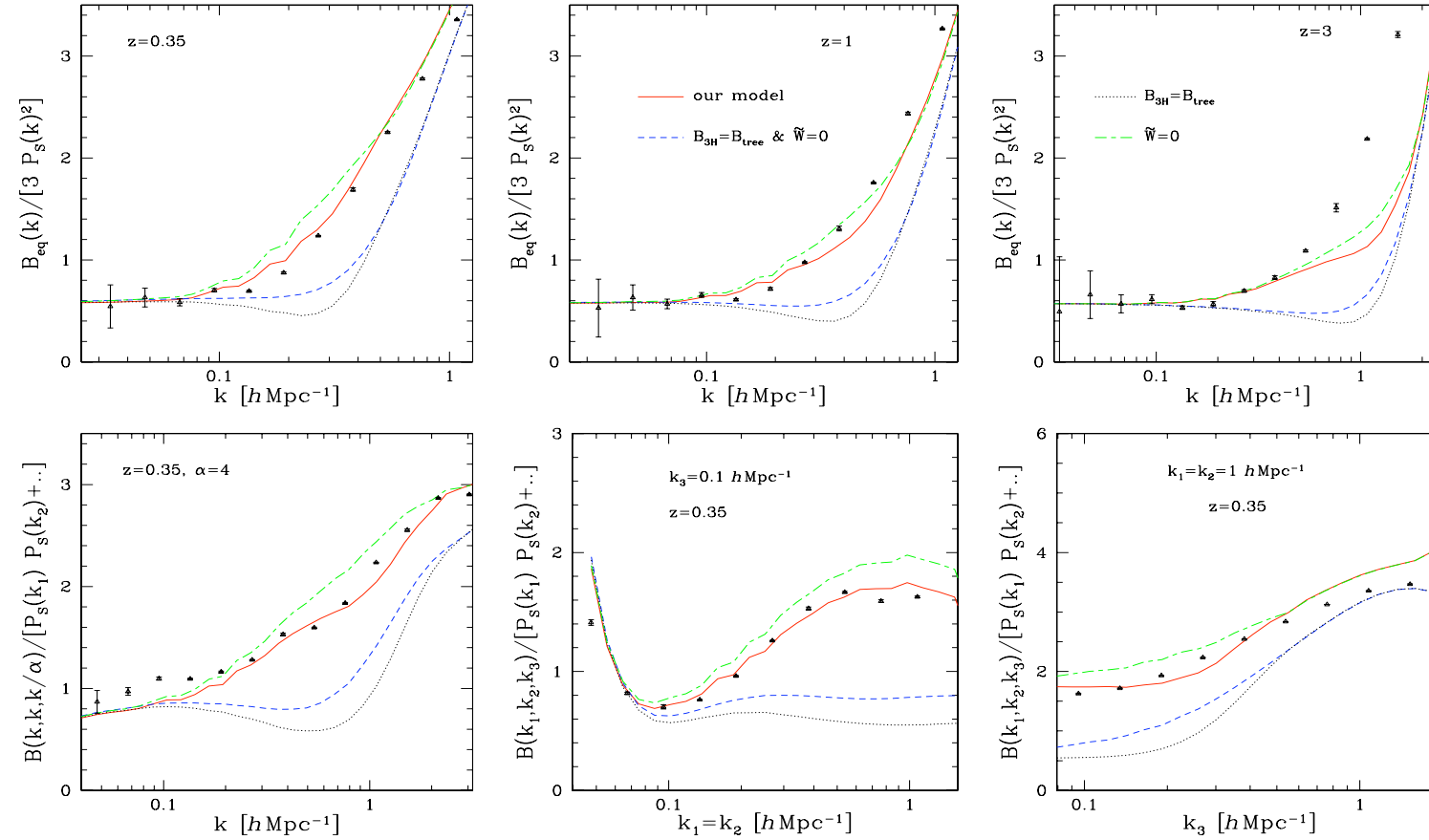


Isosceles triangles at fixed equal-sides length



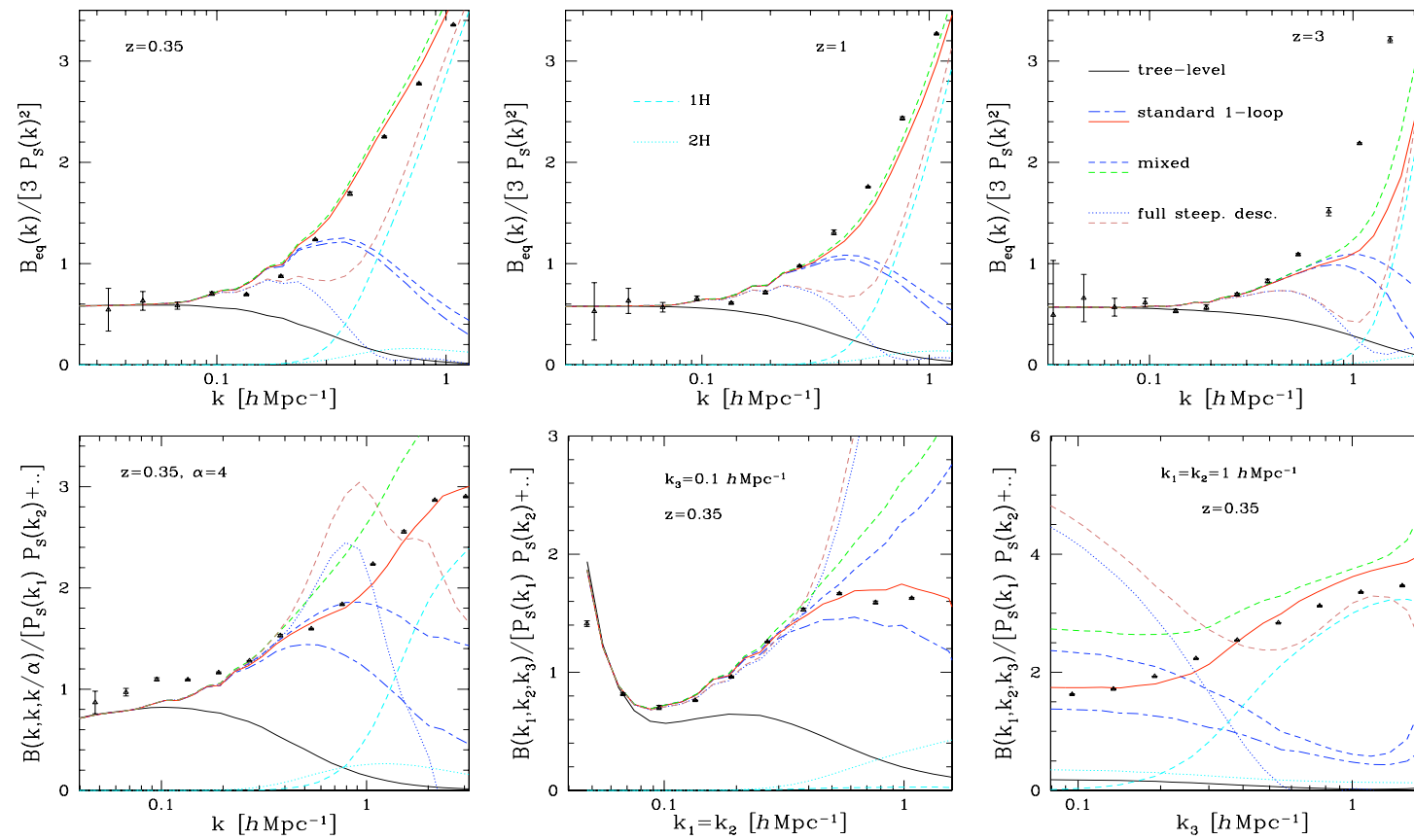
III-Dependence on various ingredients

a) Counterterms and I-loop contribution



- On these scales the counterterms do not have a great impact.
- The I-loop contribution is important.

b) Some resummation schemes ?



The 2 resummations investigated here fare worse than standard perturbation theory (1-loop order).

It may be more difficult to improve over standard perturbation theory for the bispectrum than for the power spectrum ?

Spherical collapse

In CDM, before shell-crossing, all shells move independently.

If $\epsilon(k, a)$ depends on wavenumber, all shells are coupled.

$$\ddot{r} = -\frac{4\pi G}{3} r \left[\rho_m(< r) + (1 + 3w)\bar{\rho}_{de} + \bar{\rho}_m \int_0^\infty dk 4\pi k^2 \epsilon(k) \tilde{\delta}(k) \tilde{W}(kx) \right]$$



dependence on the full density profile

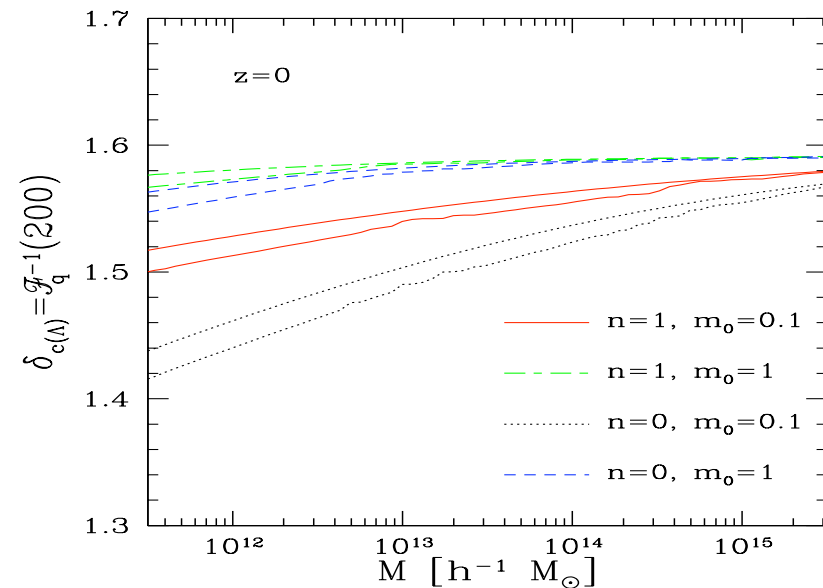
A simple approximation: use a typical profile parameterized by the shell of interest:

$$\delta(\mathbf{x}) = \frac{\delta_{x_M}}{\sigma_{x_M}^2} \int_{V_M} \frac{d\mathbf{x}'}{V_M} C_{\delta_L \delta_L}(\mathbf{x}, \mathbf{x}')$$

$$\tilde{\delta}(k) = \frac{\delta_{x_M}}{\sigma_{x_M}^2} P_L(k) \tilde{W}(kx_M)$$

This implies that the **dynamics of collapse depends on scale** (or mass).

The linear density threshold δ_c to reach a density contrast of 200 **depends on mass**.



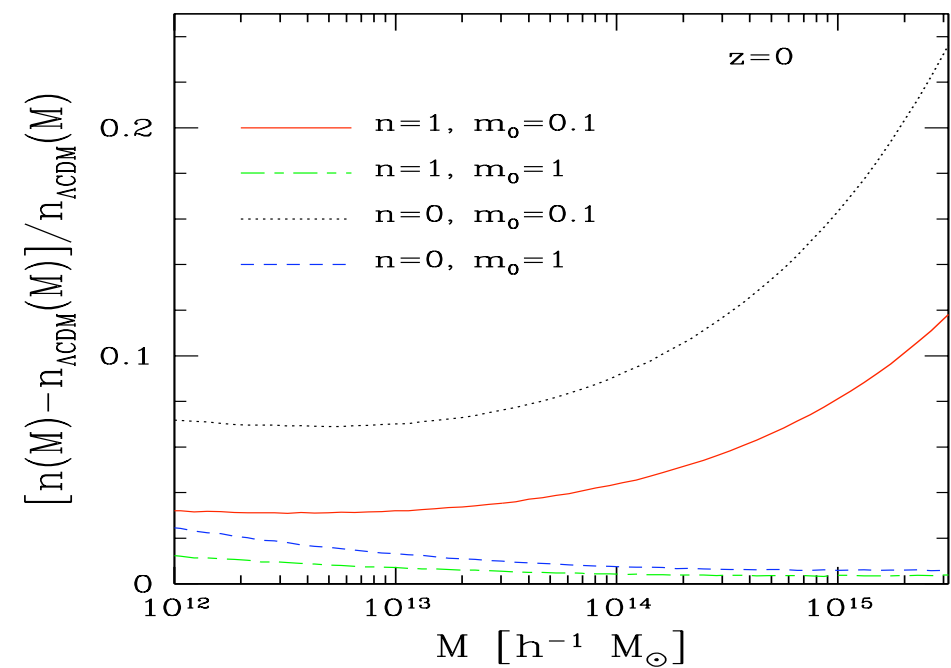
case where $\epsilon(k, a) > 0$
(mod. grav.)

Halo mass function

$$M \rightarrow \infty : \quad \ln[n(M)] \sim -\frac{\delta_c(M)^2}{2\sigma(M)^2} \quad \text{with} \quad \delta_c(M) = \mathcal{F}_q^{-1}(200)$$

Use the Press-Schechter scaling:

$$n(M) \frac{dM}{M} = \frac{\bar{\rho}_m}{M} f(\nu) \frac{d\nu}{\nu} \quad \text{with} \quad \nu = \frac{\delta_c(M)}{\sigma(M)}$$



Relative deviation of the mass function

case where $\epsilon(k, a) > 0$
(mod. grav.)

Probability distribution of the density contrast

From the spherical dynamics we can also obtain the PDF of the density contrast within spherical cells, in the weakly non-linear regime.

Introduce the cumulant generating function (Laplace transform):

$$e^{-\varphi(y)/\sigma_x^2} \equiv \langle e^{-y\delta_x/\sigma_x^2} \rangle = \int_{-1}^{\infty} d\delta_x e^{-y\delta_x/\sigma_x^2} \mathcal{P}(\delta_x)$$

$$e^{-\varphi(y)/\sigma_x^2} = (\det C_{\delta_L \delta_L}^{-1})^{1/2} \int \mathcal{D}\delta_L e^{-S[\delta_L]/\sigma_x^2}$$

where $S[\delta_L] = y \delta_x[\delta_L] + \frac{\sigma_x^2}{2} \delta_L \cdot C_{\delta_L \delta_L}^{-1} \cdot \delta_L$

On large scales, we obtain:

$$\sigma_x \rightarrow 0 : \varphi(y) \rightarrow \min_{\delta_L} S[\delta_L]$$

For spherical cells, we can look for the spherical minimum (saddle-point)

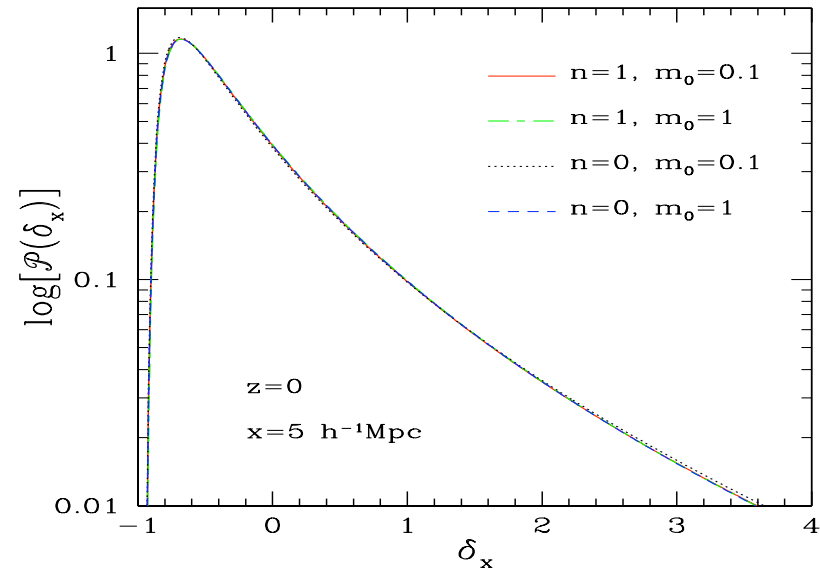
In GR the radial profile is given by:

$$\delta_{Lq'} = \delta_{Lq} \frac{\sigma_{q,q'}^2}{\sigma_q^2}$$

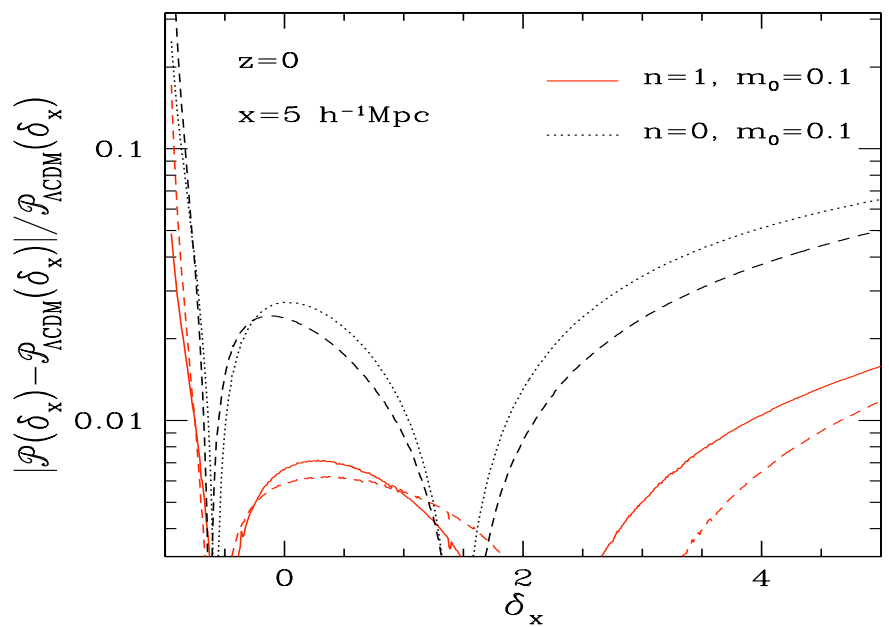
and the Lagrangian radius q associated with the Eulerian radius x is given by:

$$\begin{cases} q^3 = (1 + \delta_x) x^3 \\ \delta_x = \mathcal{F}_q(\delta_{Lq}) \end{cases}$$

This determines the Laplace transform $\varphi(y)$, whence the PDF $\mathcal{P}(\delta_x)$.



Probability distribution function



Relative deviation

case where $\epsilon(k, a) > 0$
(mod. grav.)

Modified gravity

Ph. Brax & P.V., arXiv:1205.6583

A- Definition of the model

We consider models where GR is modified through 2 scale- and time-dependent functions: $\gamma(k, a)$ and $\nu(k, a)$

Within the Newtonian gauge, $ds^2 = -a^2(1 + 2\Psi)d\tau^2 + a^2(1 - 2\Phi)d\mathbf{x}^2$,

we assume a **modified Poisson** eq.: $-k^2 \tilde{\Phi} = 4\pi \nu(k, a) G \bar{\rho}_m \tilde{\delta}/a$

and a **constitutional relation** between
the two potentials:

$$\tilde{\Psi} = \gamma(k, a) \tilde{\Phi}$$

Then, at linear order the density contrast obeys:

$$\tilde{\delta}'' + \mathcal{H}\tilde{\delta}' - \frac{3\Omega_m}{2}\mathcal{H}^2\mu(k, a)\tilde{\delta} = 0 \quad \text{with } \mu = \gamma \times \nu$$

We choose models of the form:

$$\mu(k, a) = 1 + \epsilon(k, a) \quad \text{with} \quad \epsilon(k, a) = \frac{2\beta(a)^2 k^2}{k^2 + a^2 m(a)^2}$$

This applies to chameleon and $f(R)$ models, symmetrons and dilatons.

We consider:

$$\beta(a) = \frac{1}{\sqrt{6}} \quad \text{and} \quad m(a) = m_0 a^{-3(n+2)/2}$$

Then, the density and velocity fields obey:

$$\frac{\partial \tilde{\delta}}{\partial \tau} + \tilde{\theta} = - \int d\mathbf{k}_1 d\mathbf{k}_2 \delta_D(\mathbf{k}_1 + \mathbf{k}_2 - \mathbf{k}) \alpha(\mathbf{k}_1, \mathbf{k}_2) \tilde{\theta}(\mathbf{k}_1) \tilde{\delta}(\mathbf{k}_2)$$

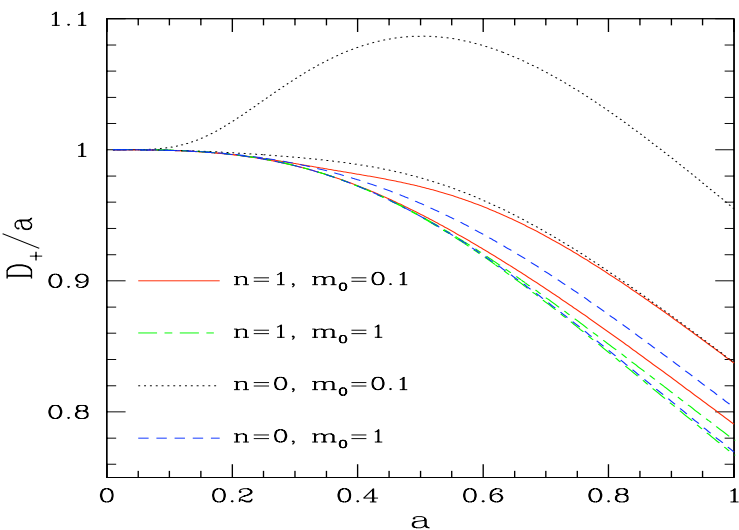
$$\frac{\partial \tilde{\theta}}{\partial \tau} + \mathcal{H}\tilde{\theta} + \frac{3\Omega_m}{2} \mathcal{H}^2 [1 + \epsilon(k, \tau)] \tilde{\delta} = - \int d\mathbf{k}_1 d\mathbf{k}_2 \delta_D(\mathbf{k}_1 + \mathbf{k}_2 - \mathbf{k}) \beta(\mathbf{k}_1, \mathbf{k}_2) \tilde{\theta}(\mathbf{k}_1) \tilde{\theta}(\mathbf{k}_2)$$

Here we neglected non-linearities in the potential and coupling functions of the scalar inducing the modification of gravity.

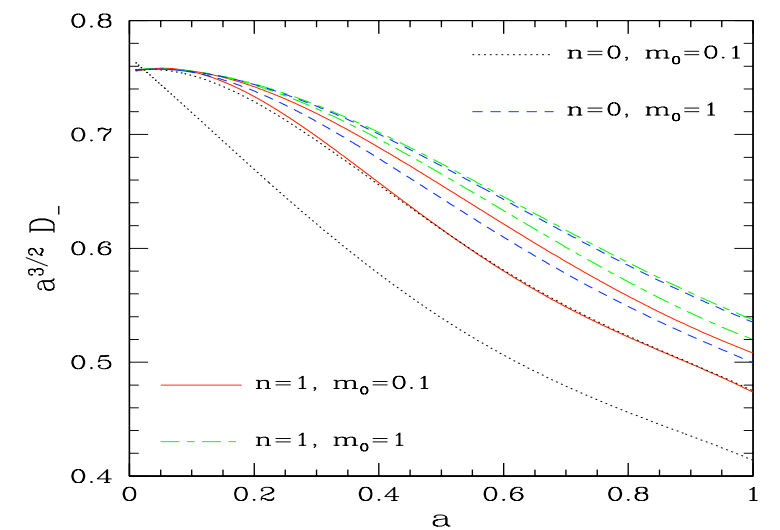
B- Linear modes

Growing mode

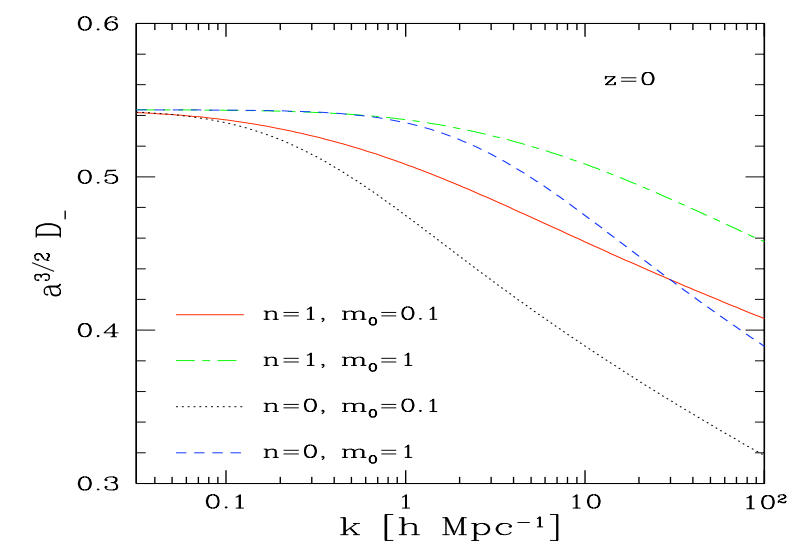
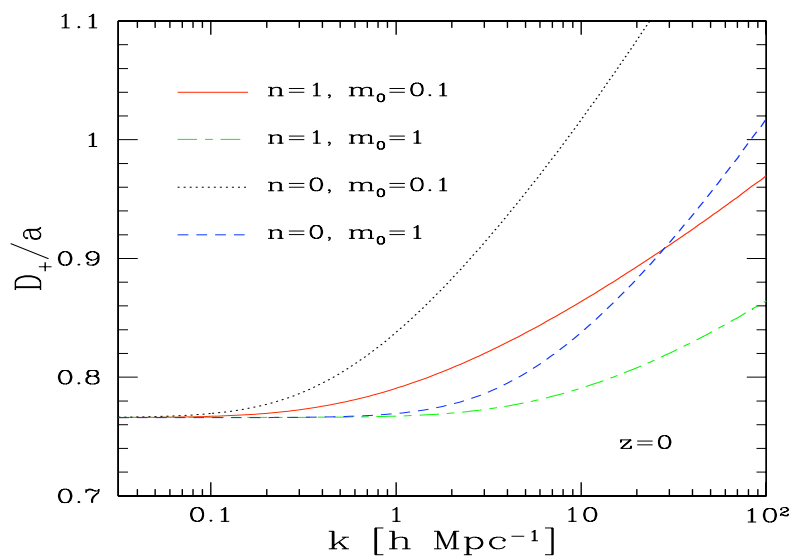
As a function of time, for
 $k=1 \text{ h/Mpc}$ and 5 h/Mpc



Decaying mode



As a function of scale,
at $z=0$.



Linear growth rate

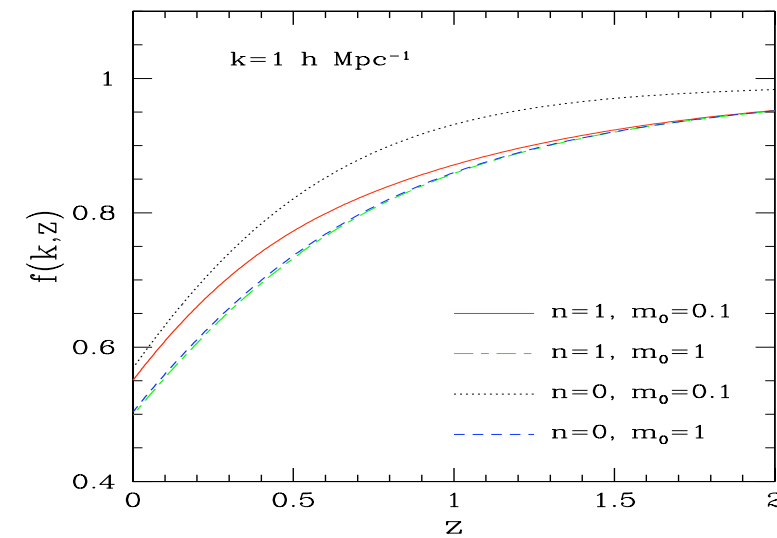
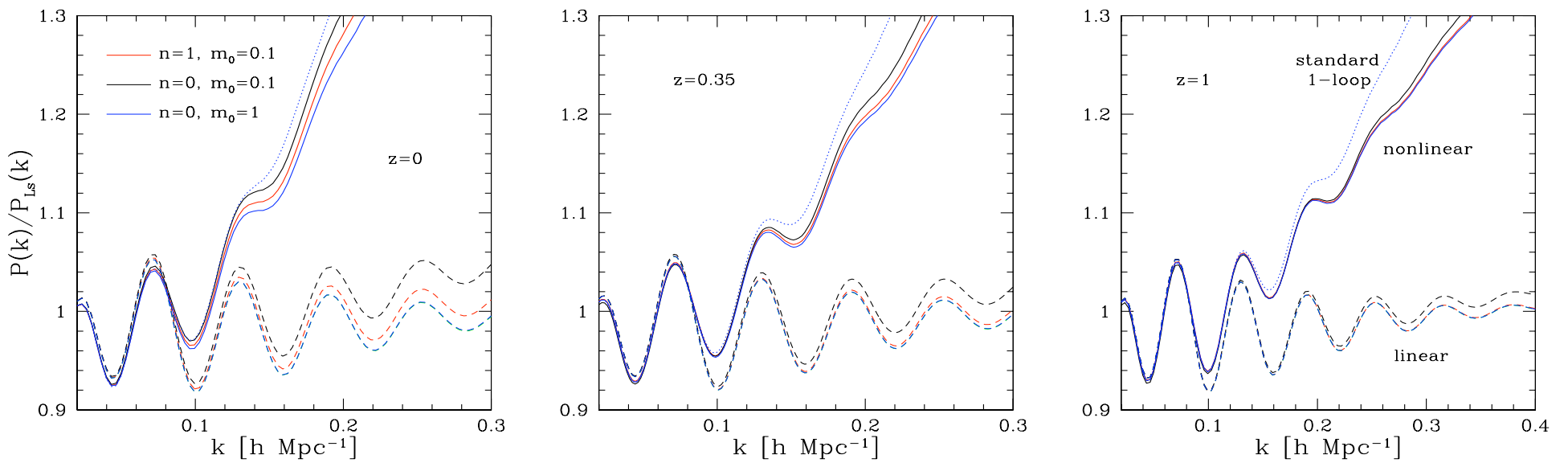


FIG. 5: Linear growth rate $f(k, z) = \partial \ln D_+ / \partial \ln a$ for wavenumber $k = 1 h \text{Mpc}^{-1}$, for four (n, m_0) models.

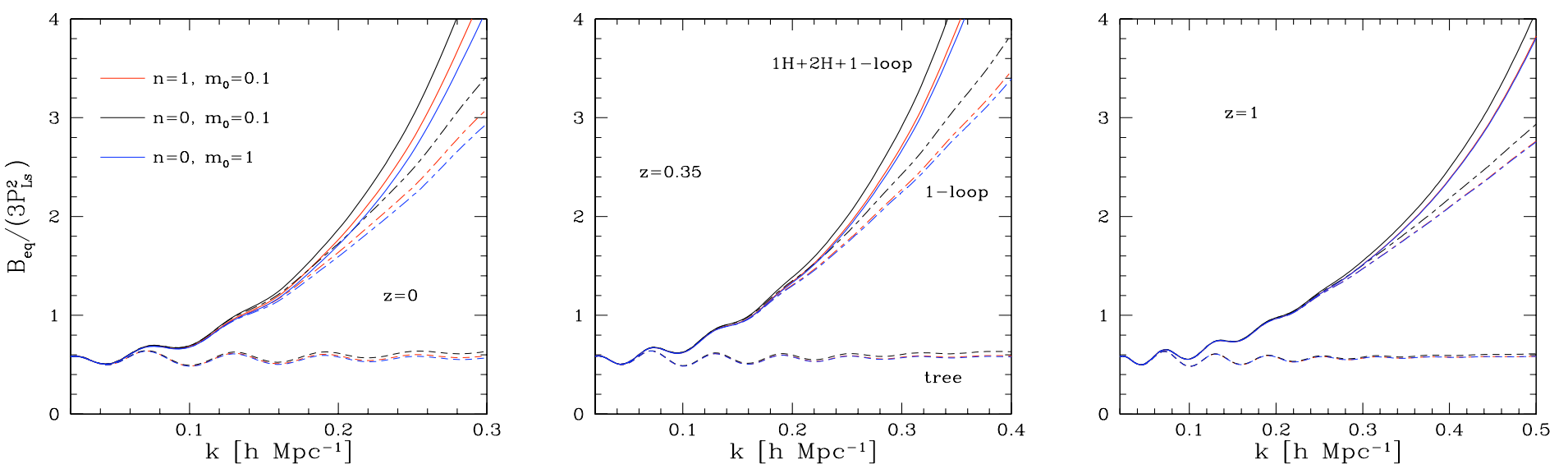
C- Perturbative regime

Power spectrum:

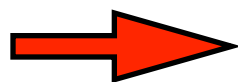


Deviations from GR are smaller or on the order of the accuracy of the standard 1-loop prediction.

Bispectrum:



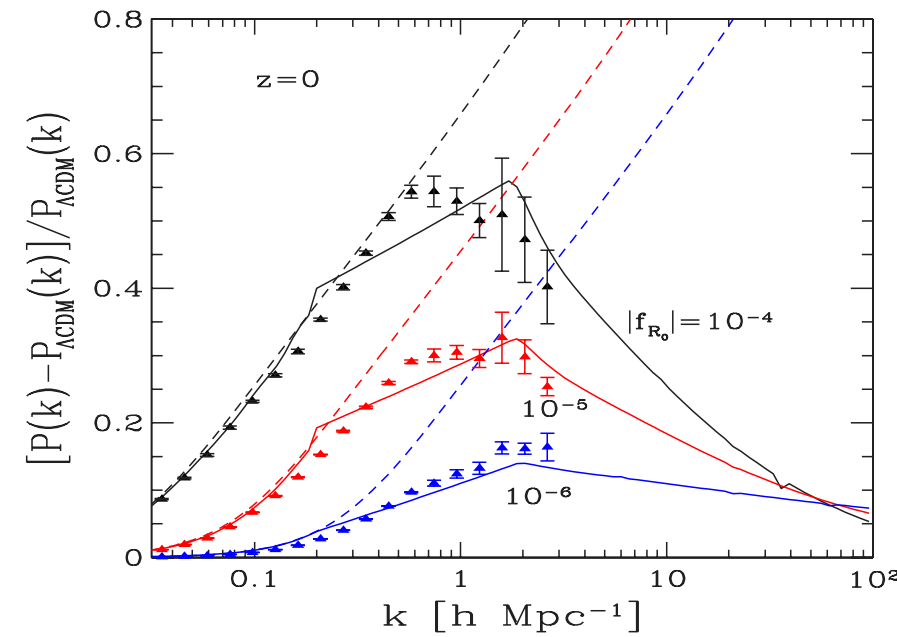
Deviations from GR are contaminated by non-perturbative terms.



The power spectrum is a more efficient/reliable probe.

D- Linear to mildly nonlinear scales

Relative deviation of the power spectrum from GR.



E- Conclusion

- realistic deviations from GR require an accuracy better than the standard 1-loop prediction.
- the bispectrum may be too sensitive to nonperturbative corrections.
- the scale-dependence of the modified-gravity kernel leads to a mass-dependent deviation from GR of the halo mass function (independently of screening effects).
- one can build reasonably efficient combined models for the power spectrum and bispectrum.